Optimal Coordination of Multiple Wind-PV-Storage Systems Considering Energy Storage-Assisted Tracking Dispatch Plans and Frequency Regulation

Junhui Li, Qinglin Sui, Wenbo Si, Xingxu Zhu, David Campos-Gaona, Fulin Fan, Ziyun Zong, and Cuiping Li

***Abstract*—To address the difficulty in recovering energy storage investment costs at renewable power plants (RPP), a collaborative optimal dispatch strategy for multiple wind-photovoltaic (PV)-storage systems is proposed, incorporating energy storage's auxiliary dispatch plan tracking and frequency regulation. It includes the optimal control strategy for wind- or PV-storage systems and the bidding-dispatching-settlement strategy for energy storage alliances participating in frequency regulation markets. The optimal energy storage control strategy aims to maximize the net profit of wind- or PV-storage system through the rolling optimization on decision-making for the energy storage output assisting in tracking the dispatch plan and delivering frequency regulation services. The bidding-dispatching-settlement strategy for energy storage alliances determines the winning capacity of each energy storage station in each frequency regulation dispatch period based on the minimum number of participating stations, and then allocates the frequency regulation tasks and benefits among the stations. The proposed strategy is verified in three particularly designed scenarios, outperforming in dispatch tracking effects and improving energy storage utilization and station economic benefits.**

***Index Terms*—energy storage, assisted tracking dispatch plan, secondary frequency regulation, frequency regulation auxiliary service market, rolling optimization.**

ABBREVIATION

CvaR	conditional value-at-risk
MPC	model predictive control
PV	photovoltaic
RPP	renewable power plants
SOC	state of charge
SMPC	stochastic model predictive control
UHVDC	ultra-high voltage direct current

Manuscript received 29 November, 2025; accepted 22 May, 2026.
(Corresponding author: Cuiping Li, e-mail: licuipingabc@163.com)

W. Si is with the Suichang County Power Supply Company, State Grid Zhejiang Electric Power, Lishui 323300, China.

D. Campos-Gaona is with the Department of Electronic and Electrical Engineering, University of Strathclyde, Glasgow G1 1XW, U.K..

F. Fan is with the School of Electrical Engineering and Automation, Harbin Institute of Technology, Harbin 150001, China.

J. Li, Q. Sui, X. Zhu, Z. Zong and C. Li are with the Key Laboratory of Modern Power System Simulation and Control Renewable Energy Technology,Ministry of Education Northeast Electric Power University, Jilin132012, China.

Color versions of one or more of the figures in this paper are available online at https://doi.org/10.26599/PEF.2026.9650009.

Digital Object Identifier 10.26599/PEF.2026.9650009

I. Introduction

To advance China's strategic goal of "building new power systems led by renewable power", renewable power represented by wind and PV power is accelerating its large-scale grid connection and replacing traditional coal-fired power units [1], [2], [3], [4], [5]. As of the end of October 2025, China's cumulative installed power generation capacity reached approximately 3750 GW, among which thermal power accounted for around 1510 GW, wind power for about 590 GW, and PV power for roughly 1140 GW [6]. The proportion of renewable power installed capacity has reached an impressive 46.13%. As regional power grids with the highest proportion of renewable power as the primary power source [7], Northwest China is endowed with abundant wind and PV resources. Due to the large power transmission volume and long transmission distance in Northwest China, the Northwest Power Grid has successively launched the UHVDC transmission mode [8]. With the large-scale grid integration of renewable power and UHVDC transmission, the active power balance level between source and load sides of power grids is declining. The frequency security and stability issues following large-power disturbances have posed significant challenges to power grids, becoming a key factor restricting the safe operation of new power systems [9], [10], [11].

Existing research focuses on the application of flexible regulating resources, such as energy storage, in frequency regulation [12]. Reference [13] pointed out that in high-proportion renewable power systems, energy storage could effectively make up for the insufficient response time of thermal power units. Reference [14] described the game relationship between energy storage and renewable power units to meet supply-demand balance and optimize the difference between revenue and cost. Reference [15] took the maximum total revenue of wind-storage combined operation as the objective, considering energy storage lifetime loss under different SOC levels and the balance between upward and downward frequency regulation capacity when energy storage participates in frequency regulation. Reference [16] integrated energy storage into PV power plants and improved the adaptive droop control strategy to maximize the frequency regulation potential of both energy storage and PV systems.

On the basis of considering the uncertainty of renewable power output, some studies have further introduced optimization methods to improve the decision-making performance of energy storage in frequency regulation. Reference [17] constructed a frequency security model for frequency support through multi-energy complementarity, and realized energy storage capacity planning via robust optimization. Although this method ensures system frequency security, robust optimization mainly considers worst-case scenarios, which might lead to resource waste and reduced efficiency. Reference [18] achieved frequency regulation by optimizing the configuration of energy storage systems, though energy storage systems which are characterized by high costs and limited lifespans require frequent maintenance and replacement. Compared with these methods, the advantage of MPC lies in its ability to continuously adjust control strategies based on the real-time system state and renewable power prediction information to cope with uncertainty [19], [20]. However, most of the above studies focus on a single RPP, and mainly consider the single scenario of energy storage supporting frequency regulation.

As the number of RPP and energy storage resources continues to increase, the issue of multi-station coordinated participation in frequency regulation has gradually attracted increasing attention. Based on the frequency regulation auxiliary service market, Ref. [21] found that regional power grids would prioritize selecting and regulating high-quality frequency regulation resources such as wind and PV power, and established a multi-source coordinated control method aimed at improving the system's dynamic response performance. By addressing different types of energy storage power stations in power grids, Ref. [22] introduced a resistance coefficient related to the remaining frequency regulation capacity of energy storage stations, which, together with frequency regulation costs, constituted the objective function, and realized the optimal allocation of frequency responses based on frequency regulation costs and remaining frequency regulation capacities of different types of energy storage stations. Reference [23] proposed a distributed control strategy, which enabled the dispatching center to ensure the response speed of secondary frequency regulation control when facing multiple distributed energy storage systems, and was feasible in engineering practice. However, for station-side energy storage in RPP, the remaining capacity available for frequency regulation is jointly affected by the current dispatch plan tracking task, the SOC of the storage system, and the output direction, thereby exhibiting clear time-varying and unidirectional characteristics. In particular, in an individual wind-storage or PV-storage system, the energy storage unit can often provide only unidirectional upward regulation or unidirectional downward regulation during certain periods, making it difficult to independently satisfy the market access requirement for bidirectional regulation capability in the frequency regulation market. This, in turn, limits both the feasibility and the profit potential of RPP energy storage participating in the frequency regulation market.

A fair and efficient market operation model is an important direction of the power system reform [24]. In the context of a diversified electricity market, how RPP optimize their bidding strategies is a crucial approach to realizing cost recovery, and holds significant importance for sustainable development of RPP [25]. The Notice on Establishing and Improving the Price Mechanism for the Power Auxiliary Service Market points out that the frequency regulation market shall, in principle, adopt a single-price mechanism based on frequency regulation mileage. Each unit independently declares its frequency regulation capacity and price, and the clearing price and winning capacity are determined through market competition [26]. Reference [27] considers the CVaR of wind power frequency regulation, proposing a multi-time-scale rolling optimization model for frequency regulation market, and then conducts wind power dispatching based on comprehensive frequency regulation indicators. However, it is difficult to completely avoid the shortage of short-term frequency regulation resources caused by random wind power. Equipping RPP with energy storage is an important measure to enhance the regulating capacity of renewable power generation and improve market competitiveness [28], [29]. In the energy market, energy storage can participate in bidding competition as an independent entity or in cooperation with renewable power [30], [31]. The current research still has the following limitations. First, research on the participation of station-side energy storage in the frequency regulation ancillary service market remains relatively limited, particularly in terms of market participation mechanisms that are compatible with ultra-short-term forecasting and rolling optimization control. Second, most studies discuss energy storage-assisted dispatch plan tracking and participation in frequency regulation services separately, without fully revealing the power coupling and capacity competition between these two tasks in real-time operation. Third, for multiple geographically distributed wind-storage and PV-storage stations within a region, existing studies have not yet systematically addressed the aggregation of remaining regulation capability, joint bidding modes, or frequency regulation revenue allocation mechanisms.

This paper focuses on the requirements of station-side energy storage in RPP for assisting dispatch plan tracking and participating in frequency regulation ancillary services, and proposes a optimal coordination strategy for multiple-wind-PV-storage systems. First, a 15-min-ahead frequency regulation ancillary service market mechanism suitable for the participation of station-side energy storage in RPP is established.

Second, for wind-storage or PV-storage systems, a rolling optimization control model is developed that considers the energy storage-assisted dispatch plan tracking and participation in frequency regulation services. Finally, a bidding–dispatching–settlement strategy for energy storage alliances participating in the frequency regulation market is proposed.

II. Coordinated Optimal Dispatch Framework for Multiple Wind-PV-Storage Systems

Based on the market mechanism of the Electric Reliability Council of Texas (ERCOT) and combined with China's general market model, this paper constructs a 15-min pre-dispatch frequency regulation ancillary service market. Different from the existing market clearing mechanisms, market participants are required to submit data such as bid capacity, capacity price bid, and mileage price bid 15 min in advance. The market completes initial clearing within 15 min with the goal of minimizing costs, considering historical frequency regulation performance indicators, and final clearing is completed after verification by the dispatching center. In the actual operation process, the dispatching center arranges the winning units to provide power frequency regulation ancillary services with a 15-min dispatch cycle based on the final clearing results. The 15-min pre-dispatch frequency regulation market can better reflect real-time supply and demand conditions and will encourage a large number of small and medium-sized power market participants to engage in frequency regulation services. To ensure the market clearing calculation performance and facilitate the dispatching of the dispatching center, only market participants with bidirectional frequency regulation capability based on a certain benchmark value for their bid capacity are allowed to participate in bidding.

The 15-min pre-dispatch frequency regulation market is highly consistent with the ultra-short-term prediction model of RPP, providing an opportunity platform for the energy storage of RPP to participate in the frequency regulation ancillary service market. To address the difficulty of unidirectional remaining regulation capacity of energy storage in wind-storage or PV-storage systems participating in the market during different time periods, an alliance-based market participation method is proposed. The energy storage alliance agent combines the directions of remaining regulation capacity of energy storage from multiple scattered RPP in the region. For the frequency regulation ancillary service market, the energy storage alliance is equivalent to an independent energy storage entity and can accept direct dispatching from the dispatching center.

This paper proposes a coordinated optimal dispatch strategy for multi-wind-PV-storage systems considering energy storage assisting in tracking dispatch plans and participating in frequency regulation. The strategy mainly consists of two parts: the optimal control strategy for energy storage in wind-storage or PV-storage systems, and the bidding–dispatching–settlement strategy for energy storage alliances participating in the frequency regulation market, as shown in Fig. 1.

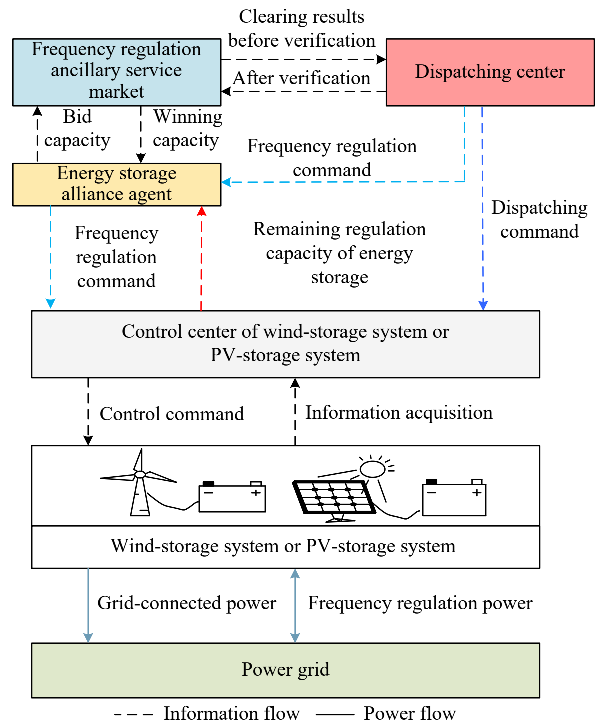

Fig. 1. Coordinated optimal dispatch schematic diagram of the multiple wind-PV-storage system.

(1) Energy storage in wind-storage or PV-storage systems operates with the primary objective of tracking dispatch plans and the secondary objective of participating in frequency regulation ancillary services. Considering the ultra-short-term predicted output of wind power or PV power, the plant control center determines the current output power of energy storage for assisting in dispatch plans and the bid power for participating in frequency regulation ancillary services in the next period, with the goal of maximizing the expected profit of the plant.

(2) With the aim of maximizing the bid capacity, the energy storage alliance agent integrates the magnitude and direction of the bid power from each energy storage unit to determine the final bid capacity for the frequency regulation ancillary service market. During the frequency regulation dispatch phase, the energy storage alliance agent directly receives frequency regulation commands from the dispatching center and distributes these commands to each energy storage unit. At the end of each dispatch cycle, settlement is conducted based on the actual profit.

III. Optimal Control Strategy for Energy Storage of the Wind- or PV-Storage System

A. Rolling Optimization Control Strategy for the Wind- or PV-Storage System

Considering that the energy storage control strategy is almost the same between wind- and PV-storage systems except for power outputs of the two different RPP types, this paper elaborates on the optimal control strategy for energy storage in RPP using the wind-storage system as an example. This study does not consider the formation method of the day-ahead generation schedule; instead, it focuses primarily on the optimal control of energy storage assisting the units in tracking dispatch plans during the intraday period and energy storage responding to frequency regulation dispatch in the real-time phase. The rolling optimization control framework of the wind-storage system is shown in Fig. 2.

(1) Stage of day-ahead generation schedule formulation: Take the day-ahead predicted output of the wind farm as the day-ahead generation schedule of the wind farm.

(2) Stage of intraday rolling optimization dispatch: To compensate for the deviation between the actual wind power output and the wind power dispatch plan output every 15 min and participate in the capacity bidding of the frequency regulation ancillary service market, based on the actual wind power output, ultra-short-term predicted output, and wind farm dispatch plan output at the current moment, considering the SOC of energy storage, with the goal of maximizing the expected profit of the wind-storage system, the rolling optimization control strategy based on MPC is adopted. By considering the current 15-min interval and the subsequent three 15-min intervals, the power of the energy storage assisting the unit in tracking the dispatch plan at the current moment and the pre-bid power of the energy storage participating in the frequency regulation ancillary service market at the next moment are determined. That is, the winning capacity of the energy storage participating in the frequency regulation ancillary service market at the current moment is determined by the previous moment, as shown in the block diagram on the right of Fig. 2. To highlight the mechanism of the proposed coordinated optimal dispatch and alliance bidding strategy, the original case study is first analyzed under ideal forecasting conditions, where the actual output is used in place of the ultra-short-term forecast output to construct the benchmark scenario. On this basis, scenarios with different levels of ultra-short-term forecast error are further introduced to conduct a sensitivity analysis of the tracking dispatch performance and economic performance of the proposed strategy.

(3) Stage of real-time frequency regulation dispatch: The stage of energy storage real-time frequency regulation dispatch is carried out simultaneously with the stage of assisting in tracking the dispatch plan. Taking the output power of the energy storage assisting the unit in tracking the dispatch plan as the reference value, considering the energy storage output direction, rated power, and SOC constraints in the same period, the energy storage takes 1 min as a response cycle and 15 min as a complete dispatch cycle to respond in real time to the frequency regulation commands issued by the energy storage alliance agent.

To further clarify the temporal coupling between rolling optimization and frequency regulation market decisions, the realized values and forecast values of the decision variables in the rolling optimization process are described in a tabular form, as shown in Table 1.

B. Construction of Optimal Operation Model for Wind-Storage System

Based on the rolling optimization control strategy for the wind-storage system proposed in Section III-A, this section constructs an optimal operation model for the wind-storage system, aiming to make optimal decisions on the output power of energy storage assisting in tracking the dispatch plan and that of energy storage participating in the frequency regulation ancillary service market during the rolling optimization process.

B.1 Objective Function

For the wind-storage system, its goal is to maximize net

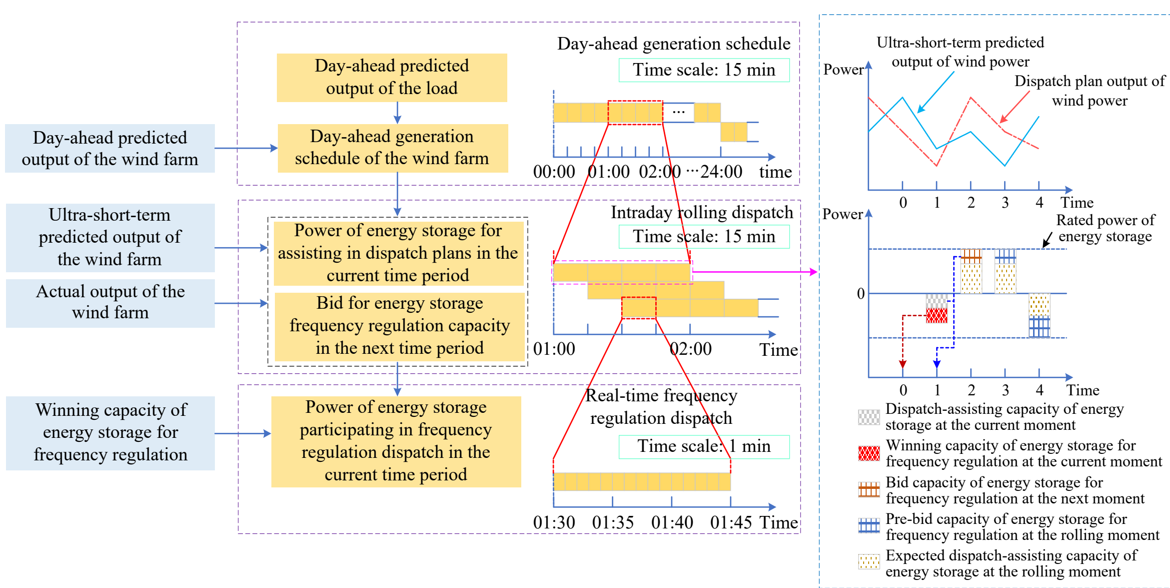

Fig. 2. Wind-storage systemr Rolling optimization control strategy framework.

TABLE 1
REALIZED AND FORECAST VALUES IN ROLLING OPTIMIZATION

Decision variables	Realized value	Forecast value
P_i^{B}	$P_i^{\mathrm{B,c}}(t)$, $P_i^{\mathrm{B,d}}(t)$	$P_i^{\mathrm{B,c}}(t+1:t+3)$ $P_i^{\mathrm{B,d}}(t+1:t+3)$
C^{bid}	$P_i^{\mathrm{B,up}}(t+1)$, $P_i^{\mathrm{B,down}}(t+1)$	$P_i^{\mathrm{B,up}}(t+2:t+3)$ $P_i^{\mathrm{B,down}}(t+2:t+3)$
f_i	$f_i^{\mathrm{c}}(t)$, $f_i^{\mathrm{d}}(t)$	$f_i^{\mathrm{c}}(t+1:t+3)$ $f_i^{\mathrm{d}}(t+1:t+3)$
SOC_i	$\mathrm{SOC}_i(t)$	$\mathrm{SOC}_i(t+1:t+3)$

profit, so the objective function of the optimal control model is as shown in Eq. (1). The income of the wind-storage system includes income from on-grid electricity, frequency regulation capacity income and frequency regulation mileage income; the cost includes energy storage life loss cost, energy loss cost, and output deviation penalty cost.

$$\begin{cases} W_i^{\mathrm{P}} = \max \sum_{t=1}^{T} (W_i^{\mathrm{R}}(t) - W_i^{\mathrm{C}}(t)) \\ W_i^{\mathrm{R}}(t) = W_i^{\mathrm{R,E}}(t) + W_i^{\mathrm{R,C}}(t) + W_i^{\mathrm{R,M}}(t) \\ W_i^{\mathrm{C}}(t) = W_i^{\mathrm{C,L}}(t) + W_i^{\mathrm{C,E}}(t) + W_i^{\mathrm{C,D}}(t) \end{cases} \tag{1}$$

where W_i^{P} denotes the profit of wind-storage system i within the total number of current rolling optimization time periods; T denotes the total number of current rolling optimization time periods; $W_i^{\mathrm{R}}(t)$ and $W_i^{\mathrm{C}}(t)$ respectively denote the income and cost of wind-storage system i in time period t; $W_i^{\mathrm{R,E}}(t)$, $W_i^{\mathrm{R,C}}(t)$, and $W_i^{\mathrm{R,M}}(t)$ respectively denote the income from on-grid electricity, frequency regulation capacity income, and frequency regulation mileage income of wind-storage system i in time period t; $W_i^{\mathrm{C,L}}(t)$ and $W_i^{\mathrm{C,E}}(t)$ respectively denote the life loss cost and energy loss cost of the energy storage of wind-storage system i in time period t; and $W_i^{\mathrm{C,D}}(t)$ denotes the output deviation penalty cost of wind-storage system i in time period t.

(1) Income from on-grid electricity of wind-storage system

The wind-storage system obtains power generation compensation when it integrates the generated electricity into the power grid, and the income from on-grid electricity of the wind-storage system in time period t is

$$\begin{cases} W_i^{\mathrm{R,E}}(t) = \lambda P_i^{\mathrm{WB}}(t) \triangle t \\ P_i^{\mathrm{WB}}(t) = P_i^{\mathrm{W}}(t) + P_i^{\mathrm{B,c}}(t) - P_i^{\mathrm{B,d}}(t) \end{cases} \tag{2}$$

where λ denotes the on-grid price; $P_i^{\mathrm{WB}}(t)$ denotes the combined output of wind-storage system i in time period t; $P_i^{\mathrm{W}}(t)$ denotes the actual output of the unit of wind-storage system i in time period t; and $P_i^{\mathrm{B,c}}(t)$ and $P_i^{\mathrm{B,d}}(t)$ respectively denote the charging and discharging power of the energy storage assisting the unit of wind-storage system i in tracking the dispatch plan in time period t.

(2) Frequency regulation capacity income and frequency regulation mileage income of wind-storage system

Under the general electricity market rules in China, energy storage receives frequency regulation capacity compensation and frequency regulation mileage compensation when participating in the frequency regulation ancillary service market, and the frequency regulation ancillary service income of the wind-storage system in time period t is

$$\begin{cases} W_i^{\mathrm{R,C}}(t) = B^{\mathrm{C}} P_i^{\mathrm{B,C}}(t) \\ W_{t,i}^{\mathrm{R,M}} = B^{\mathrm{M}} K_i(t) P_i^{\mathrm{B,M}}(t) \end{cases} \tag{3}$$

where B^{C} and B^{M} respectively denote the frequency regulation capacity price and the frequency regulation mileage price; $P_i^{\mathrm{B,C}}(t)$ and $P_i^{\mathrm{B,M}}(t)$ denote the winning frequency regulation capacity and the actual frequency regulation mileage of the energy storage of wind-storage system i in time period t, respectively; and $K_i(t)$ denotes the frequency regulation performance of wind-storage system i in time period t.

Generally speaking, energy storage can respond quickly to frequency regulation commands, and the frequency regulation performance of wind-storage system i in time period t can be simplified as a piecewise function related to the SOC of energy storage, as follows

$$K_i(t) = \begin{cases} 1.8, 0.2 \leqslant \mathrm{SOC}_i(t) \leqslant 0.8 \\ 1, \quad \text{else} \end{cases} \tag{4}$$

where $\mathrm{SOC}_i(t)$ denotes the ratio of the remaining energy to the full charge capacity of energy storage i at the start of time period t.

This paper adopts a piecewise function to approximately characterize this relationship. This treatment preserves physical interpretability while also facilitating the solution of the rolling optimization model. The specific details can be found in Ref. [32].

(3) Life loss cost of energy storage

To more accurately reflect the differences in battery lifetime degradation under different depths of charge and discharge, this paper extends the original linear lifetime loss model to a degradation model considering cycle depth. Specifically, the equivalent cycle depth is first extracted from the energy storage SOC sequence, as shown in Eq. (5); then, a power-function relationship between cycle life and cycle depth is adopted to describe the battery lifetime characteristics, as shown in Eq. (6). On this basis, the lifetime degradation cost caused by a single cycle is expressed by Eq. (7). Therefore, the total lifetime degradation cost of the energy storage system i in time period t of the dispatch horizon is given by Eq. (8).

$$\mathrm{DoD}_{k,i}(t) = \mathrm{SOC}_{k,i}^{\max}(t) - \mathrm{SOC}_{k,i}^{\min}(t) \tag{5}$$

$$N(\mathrm{DoD}_{k,i}(t)) = N_{100,i} \mathrm{DoD}_{k,i}^{-b}(t) \tag{6}$$

$$W_{k,i}^{C,L}(t) = \frac{C_{\mathrm{inv},i}}{N(\mathrm{DoD}_{k,i}(t))} \tag{7}$$

$$W_i^{C,L}(t) = \sum_{k=1}^{n_c} \frac{C_{\text{inv},i}}{N_{100,i}} \text{DoD}_{k,i}^b(t) \tag{8}$$

where $\text{DoD}_{k,i}(t)$ denotes the cycle depth of the energy storage system of wind-storage system i in the k^{th} cycle during period t; $N_{100,i}$ denotes the rated cycle life of the energy storage system of wind-storage system i at 100% depth of discharge; b denotes the cycle-depth influence coefficient; $N(\text{DoD}_{k,i}(t))$ denotes the battery cycle life of wind-storage system i at the cycle depth DoD_k in time period t; $C_{\text{inv},i}$ denotes the investment cost of the energy storage system of wind-storage system i; $W_{k,i}^{C,L}(t)$ denotes the lifetime degradation cost of the energy storage system of wind-storage system i in the k^{th} cycle in time period t; and n_c denotes the total number of cycles.

(4) Energy loss cost of energy storage

In actual operation, energy storage will result in a certain amount of energy loss because the charging–discharging efficiency fails to reach 100%. The energy loss cost of energy storage in time period t is

$$\begin{cases} W_i^{\text{C,E}}(t) = W_i^{\text{C,Ec}}(t) + W_i^{\text{C,Ed}}(t) \\ W_i^{\text{C,Ec}}(t) = \lambda \left[P_i^{\text{B,c}}(t) \triangle t + \beta P_i^{\text{B,down}}(t) \right] (1 - \eta_i^{\text{c}}) \\ W_i^{\text{C,Ed}}(t) = \lambda \left[P_i^{\text{B,d}}(t) \triangle t + \beta P_i^{\text{B,up}}(t) \right] \left(\dfrac{1}{\eta_i^{\text{d}}} - 1 \right) \end{cases} \tag{9}$$

where $W_i^{\text{C,Ec}}(t)$ and $W_i^{\text{C,Ed}}(t)$ respectively denote the charging–discharging energy loss cost of the energy storage of wind-storage system i in time period t; η_i^{c} and η_i^{d} respectively denote the charging efficiency and discharging efficiency of energy storage i. $P_i^{\text{B,up}}(t)$ and $P_i^{\text{B,down}}(t)$ respectively denote the upward frequency regulation power and downward frequency regulation power of energy storage i in time period t; and β denotes the frequency regulation energy coefficient, indicating that the energy storage will charge (discharge) β MWh of energy in actual operation for every 1 MW of frequency regulation power provided.

(5) Output deviation penalty cost of wind-storage system

When the actual power generation of the wind-storage system fails to meet the dispatch plan requirements, the market dispatch authority will impose a deviation penalty based on the power shortage; when the actual power generation exceeds the dispatch plan requirements, it will lead to wind curtailment, resulting in economic losses for the power station. During the rolling optimization operation of the wind-storage system, this part of the cost must be minimized as much as possible, and the output deviation penalty cost of the wind-storage system in time period t is

$$W_i^{\text{C,D}}(t) = 2\lambda \left| P_i^{\text{WB}}(t) - P_i^{\text{WP}}(t) \right| \tag{10}$$

where $P_i^{\text{WP}}(t)$ denotes the dispatch plan output of the unit i in time period t.

B.2 Constraints

The constraints of the optimization model mainly include energy storage constraints and wind-storage system power generation constraints.

(1) Energy storage constraints

Energy storage will be subject to power constraints and energy constraints in actual operation.

Energy storage power constraints include power constraints when assisting the unit in tracking the dispatch plan and power constraints for participating in frequency regulation. It is stipulated that the energy storage's dispatch plan tracking output shall not exceed its rated power; the sum of the dispatch plan tracking output and the frequency regulation participation power of energy storage shall not exceed its rated power; energy storage is only allowed to operate in the charging state or discharging state during the same dispatch period. Details are as follows

$$\begin{cases} 0 \leqslant P_i^{\text{B,c}}(t) \leqslant f_i^{\text{c}}(t) P_i^{\text{B,rate}} \\ 0 \leqslant P_i^{\text{B,d}}(t) \leqslant f_i^{\text{d}}(t) P_i^{\text{B,rate}} \\ 0 \leqslant P_i^{\text{B,c}}(t) + P_i^{\text{B,down}}(t) \leqslant f_i^{\text{c}}(t) P_i^{\text{B,rate}} \\ 0 \leqslant P_i^{\text{B,d}}(t) + P_i^{\text{B,up}}(t) \leqslant f_i^{\text{d}}(t) P_i^{\text{B,rate}} \\ f_i^{\text{c}}(t) + f_i^{\text{d}}(t) \leqslant 1 \\ f_i^{\text{c}}(t), f_i^{\text{d}}(t) \in \{0, 1\} \end{cases} \tag{11}$$

where $f_i^{\text{c}}(t)$ and $f_i^{\text{d}}(t)$ respectively denote the binary variables for charging and discharging of energy storage i in time period t; and $P_i^{\text{B,rate}}$ denotes the rated power of energy storage i.

The main purpose of energy storage's energy constraints is to avoid life degradation caused by overcharging and over discharging of energy storage, so it is necessary to impose certain restrictions on its depth of charge and discharge during operation. Details are as follows

$$\begin{cases} \text{SOC}_i^{\min} \leqslant \text{SOC}_i(t) \leqslant \text{SOC}_i^{\max} \\ \text{SOC}_i(t) = \text{SOC}_i(t-1) + \triangle\text{SOC}_i(t) \\ \triangle\text{SOC}_i(t) = \\ \dfrac{\eta_i^{\text{c}} \left[P_i^{\text{B,c}}(t) \triangle t + \beta P_i^{\text{B,down}}(t) \right] - \dfrac{P_i^{\text{B,d}}(t) \triangle t + \beta P_i^{\text{B,up}}(t)}{\eta_i^{\text{d}}}}{E_i^{\text{B,rate}}} \end{cases} \tag{12}$$

where $\text{SOC}_i^{\min}$ and $\text{SOC}_i^{\max}$ respectively denote the minimum and maximum values of the SOC of energy storage i; $\text{SOC}_i(t)$ denotes the SOC of energy storage i in time period t; $\text{SOC}_i(t-1)$ denotes the SOC of energy storage i in time period $t-1$; $\triangle\text{SOC}_i(t)$ denotes the SOC variation of energy storage i in time period t; and $E_i^{\text{B,rate}}$ denotes the rated capacity of energy storage i.

(2) Wind-storage system power generation constraints

To ensure the safe and stable operation of the power grid, the actual on-grid electricity of the wind-storage system shall strictly follow the dispatch plan. However, wind power output exhibits significant uncontrollability and volatility, making it difficult to achieve precise output in accordance with the dispatch plan. Meanwhile, the "Detailed Rules for the Administration of Power Grid Connection and Operation in the North China Region" stipulates that units with a single-machine capacity of 100 MW or less are exempt from penalties if the dispatch deviation is less than 3%. Based on this provision, this paper sets an allowable error range for the dispatch plan of the wind-storage system, and the combined output of the wind-storage system within this range shall be deemed to operate in accordance with the dispatch plan. Details are as follows

$$\begin{cases} P_i^{\mathrm{WP,up}}(t) = (1+\theta)P_i^{\mathrm{WP}}(t) \\ P_i^{\mathrm{WP,down}}(t) = (1-\theta)P_i^{\mathrm{WP}}(t) \end{cases} \tag{13}$$

where $P_i^{\mathrm{WP,up}}(t)$ and $P_i^{\mathrm{WP,down}}(t)$ respectively denote the upper and lower limits of the combined power generation of wind-storage system i in time period t; and θ denotes the allowable dispatch deviation.

After considering the allowable error range of the wind-storage system's dispatch plan output, the combined power generation constraint of the wind-storage system is

$$P_i^{\mathrm{WP,down}}(t) \leqslant P_i^{\mathrm{WB}}(t) \leqslant P_i^{\mathrm{WP,up}}(t) \tag{14}$$

When the combined output of the wind-storage system fails to enter the allowable error range of the dispatch plan in time period t, the combined power generation constraint of the wind-storage system is not considered; instead, only the allowable error range of the dispatch plan is taken into account. In actual operation, the wind-storage system will minimize the dispatch deviation due to the substantial power deviation penalty cost.

IV. Bidding-Dispatching-Settlement Strategy for Energy Storage Alliances Participating in the Frequency Regulation Market

The process of energy storage alliances participating in the frequency regulation auxiliary service market is shown in Fig. 3. Before the response period, each station within the alliance declares the size and direction of the frequency regulation capacity for the response period to the energy storage alliance agent. The energy storage alliance agent integrates the declared capacities of each energy storage station, determines the final declared capacity to the frequency regulation auxiliary service market, and feeds back their winning capacity to each station within the alliance. During the response period, the dispatching center issues frequency regulation instructions to the energy storage alliance based on the winning information provided by the frequency regulation auxiliary service market. The energy storage alliance agent allocates the frequency regulation tasks to each station within the alliance for execution in accordance with its internal dispatching strategy.

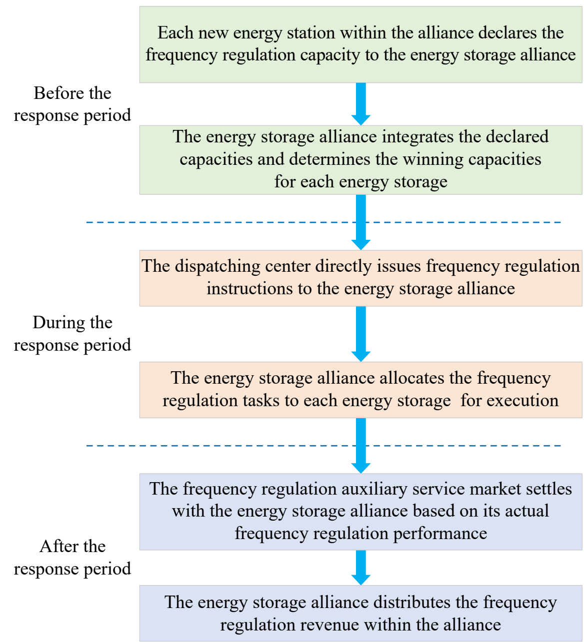

Fig. 3. Process of energy storage alliances participating in the frequency regulation auxiliary service market.

After the response period, the frequency regulation auxiliary service market settles with the energy storage alliance agent based on its actual frequency regulation performance, and the energy storage alliance agent is responsible for distributing the frequency regulation revenue to each station within the alliance.

A. Bidding Strategy Considering the Maximization of Alliance Benefits

Based on the 15-min-ahead frequency regulation auxiliary service market mechanism, the energy storage alliance agent needs to determine the bidding capacity during the bidding phase. To achieve the maximum frequency regulation auxiliary service revenue and meet the basic market access conditions, the energy storage alliance agent takes the minimum value of the sum of the upward frequency regulation power and the sum of the downward frequency regulation power declared by each station as the bidding capacity for participating in the frequency regulation auxiliary service market. The declared capacity of the energy storage alliance agent participating in the frequency regulation market after integrating the declared capacities of each station in time period t is expressed as

$$C^{\mathrm{bid}}(t) = \min\left[\sum_{i=1}^{I} P_i^{\mathrm{B,up}}(t), \sum_{i=1}^{I} P_i^{\mathrm{B,down}}(t)\right] \tag{15}$$

where $C^{\mathrm{bid}}(t)$ denotes the bidding capacity of the energy storage alliance agent for participating in the frequency regulation auxiliary service market in time period t, and I denotes the number of stations participating in the energy storage alliance.

After the energy storage alliance agent determines the bidding capacity for the response period, it needs to promptly notify each station within the alliance of their actual winning capacity. This allows each station to adjust the energy storage power reserved for responding to frequency regulation tasks during the response period, thereby improving the ability of energy storage auxiliary units within the station to track the dispatched output. Each station in the energy storage alliance maintains a cooperative–competitive relationship. If a station's declared capacity includes both upward and downward frequency regulation power, it can directly participate in the frequency regulation auxiliary service market without joining the alliance. Therefore, when determining the actual winning capacity of each station within the alliance, priority should be given to ensuring the winning of the equivalent bidirectional partial capacity for such stations. For dispatch convenience, the winning capacity of stations that only declare unidirectional frequency regulation power and the remaining declared power of the aforementioned stations is determined based on the minimum number of participants.

If a station's declared capacity includes both upward and downward frequency regulation power, its equivalent bidirectional partial capacity is guaranteed to win; otherwise, its guaranteed winning capacity is zero. Details are as follows

$$C_i^{\text{bid,must}}(t) = \begin{cases} \min\left[P_i^{\text{B,up}}(t), P_i^{\text{B,down}}(t)\right], P_i^{\text{B,up}}(t) > 0 \text{ and } P_i^{\text{B,down}}(t) > 0 \\ 0, \quad \text{else} \end{cases} \tag{16}$$

where $C_i^{\text{bid,must}}(t)$ denotes the guaranteed winning capacity of station i in time period t, including upward frequency regulation power and downward frequency regulation power. The deficit capacity of the energy storage alliance agent in time period t after subtracting the sum of the guaranteed winning capacities of each station is

$$C_i^{\text{need}}(t) = C^{\text{bid}}(t) - \sum_{i=1}^{I} C_i^{\text{bid,must}}(t) \tag{17}$$

where $C_i^{\text{need}}(t)$ denotes the sum of the frequency regulation capacity to be additionally provided by each station within the alliance, including upward frequency regulation power and downward frequency regulation power.

The remaining available upward power and downward power of each station within the alliance after subtracting the guaranteed winning capacity from the declared capacity are

$$\begin{cases} C_i^{\text{sur,up}}(t) = P_i^{\text{B,up}}(t) - C_i^{\text{bid,must}}(t) \\ C_i^{\text{sur,down}}(t) = P_i^{\text{B,down}}(t) - C_i^{\text{bid,must}}(t) \end{cases} \tag{18}$$

where $C_i^{\text{sur,up}}(t)$ and $C_i^{\text{sur,down}}(t)$ respectively denote the remaining available upward frequency regulation power and downward frequency regulation power of station i in time period t.

To ensure the minimum number of participants in each frequency regulation dispatch period of the energy storage alliance, both the remaining available upward and downward frequency regulation power of each station in the alliance are sorted in descending order. The sum is accumulated from top to bottom until the total upward frequency regulation power and total downward frequency regulation power of the selected stations both meet the deficit capacity. At this point, part or all of the remaining capacity of the selected stations wins the bid, while the remaining capacity of the other stations fails to win the bid.

The actual winning capacity of station i within the alliance in time period t is

$$\begin{cases} C_i^{\text{bid,up}}(t) = C_i^{\text{bid,must}}(t) + C_i^{\text{sup,up}}(t) \\ C_i^{\text{bid,down}}(t) = C_i^{\text{bid,must}}(t) + C_i^{\text{sup,down}}(t) \end{cases} \tag{19}$$

where $C_i^{\text{bid,up}}(t)$ denotes the winning upward frequency regulation capacity of Station i in time period t; $C_i^{\text{bid,down}}(t)$ denotes the winning downward frequency regulation capacity of station i in time period t; $C_i^{\text{sup,up}}(t)$ denotes the winning part of the remaining available upward frequency regulation power of station i in time period t; and $C_i^{\text{sup,down}}(t)$ denotes the winning part of the remaining available downward frequency regulation power of station i in time period t.

B. Dispatching Strategy Considering Equal Opportunity of Frequency Regulation Response for Stations

During the response period, the energy storage alliance agent receives frequency regulation instructions issued by the dispatch center and allocates frequency regulation tasks in proportion to the actual winning upward and downward frequency regulation capacities of each station. The frequency regulation task that station i shall undertake during the j^{th} frequency regulation dispatch in time period t is

$$P_{i,j}^{\text{AGC}}(t) = \begin{cases} \dfrac{C_i^{\text{bid,up}}(t)}{\sum_{i=1}^{I} C_i^{\text{bid,up}}(t)} P_j^{\text{AGC}}(t), & P_j^{\text{AGC}}(t) > 0 \\ 0, & P_j^{\text{AGC}}(t) = 0 \\ \dfrac{C_i^{\text{bid,down}}(t)}{\sum_{i=1}^{I} C_i^{\text{bid,down}}(t)} P_j^{\text{AGC}}(t), & P_j^{\text{AGC}}(t) < 0 \end{cases} \tag{20}$$

where $P_{i,j}^{\text{AGC}}(t)$ denotes the frequency regulation task that station i shall undertake during the j^{th} frequency regulation dispatch in time period t, and $P_j^{\text{AGC}}(t)$ denotes the frequency regulation instruction received by the energy storage alliance agent during the j^{th} dispatch in time period t.

C. Settlement Strategy Based on the Process of Actual Frequency Regulation Response of Stations

As the hub between the frequency regulation auxiliary service market and the stations, the market settles accounts based on the actual response of the energy storage alliance agent. The frequency regulation revenue obtained by the energy storage alliance agent in time period t is

$$\begin{cases} R^{\mathrm{C}}(t) = B^{\mathrm{C}} \sum_{i=1}^{I} \left[C_i^{\mathrm{bid,up}}(t) + C_i^{\mathrm{bid,down}}(t) \right] \\ R^{\mathrm{M}}(t) = B^{\mathrm{M}} K(t) \sum_{i=1}^{I} \sum_{j=1}^{J} P_{i,j}^{\mathrm{AGC}}(t) \end{cases} \tag{21}$$

where $R^{\mathrm{C}}(t)$ denotes the frequency regulation capacity revenue of the energy storage alliance agent in time period t; $R^{\mathrm{M}}(t)$ denotes the frequency regulation mileage revenue of the energy storage alliance agent in time period t; $K(t)$ denotes the frequency regulation performance of the energy storage alliance in time period t, taking the mean value of the frequency regulation performance of the stations within the alliance; and J denotes the number of frequency regulation dispatches within time period t.

Based on the winning capacity and actual dispatch situation of each station, the energy storage alliance agent allocates the frequency regulation revenue, without considering cost sharing temporarily. The frequency regulation revenue of Station i in time period t is

$$\begin{cases} R_i^{\mathrm{C}}(t) = \dfrac{C_i^{\mathrm{bid,up}}(t) + C_i^{\mathrm{bid,down}}(t)}{\sum_{i=1}^{I} \left[C_i^{\mathrm{bid,up}}(t) + C_i^{\mathrm{bid,down}}(t) \right]} R^{\mathrm{C}}(t) \\ R_i^{\mathrm{M}}(t) = \dfrac{\sum_{j=1}^{J} P_{i,j}^{\mathrm{AGC}}(t)}{\sum_{i=1}^{I} \sum_{j=1}^{J} P_{i,j}^{\mathrm{AGC}}(t)} R^{\mathrm{M}}(t) \end{cases} \tag{22}$$

where $R_i^{\mathrm{C}}(t)$ denotes the frequency regulation capacity revenue of station i in time period t, and $R_i^{\mathrm{M}}(t)$ denotes the frequency regulation mileage revenue of station i in time period t.

The overall process of the control strategy described earlier is shown in Fig. 4.

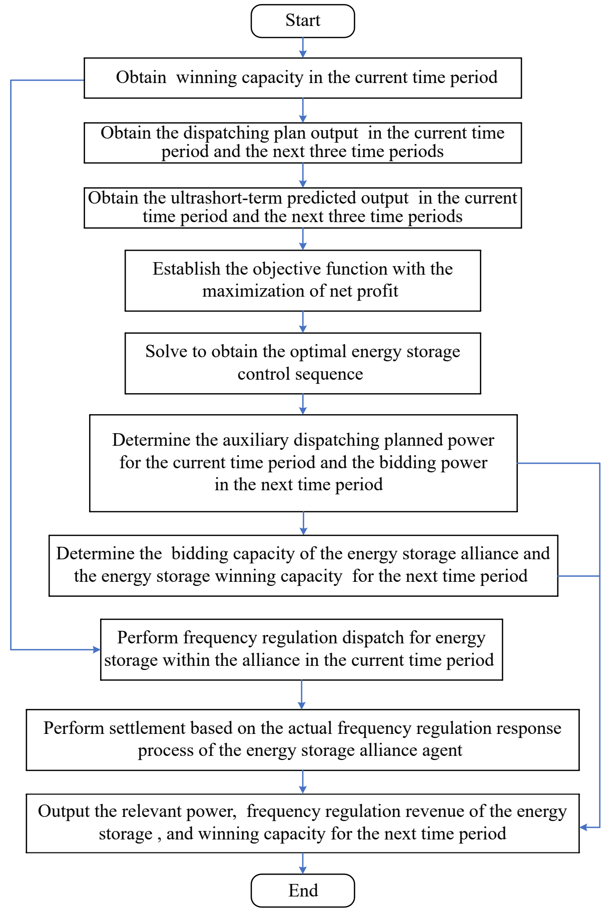

Fig. 4. Control strategy flow chart.

D. Evaluation Indicators

(1) Performance indicator for tracking dispatching plans

$$P_i^{\mathrm{index}} = \frac{1}{100} \sqrt{\frac{\sum_{t=1}^{T} (P_i^{\mathrm{err}}(t))^2}{T}} \tag{23}$$

$$P_i^{\mathrm{err}}(t) = \begin{cases} P_i^{\mathrm{WB}}(t) - P_i^{\mathrm{WP,up}}(t), & P_i^{\mathrm{WB}}(t) > P_i^{\mathrm{WP,up}}(t) \\ P_i^{\mathrm{WP,down}}(t) - P_i^{\mathrm{WB}}(t), & P_i^{\mathrm{WP,down}}(t) > P_i^{\mathrm{WB}}(t) \\ 0, & \text{else} \end{cases} \tag{24}$$

where P_i^{index} denotes the performance indicator for station i to track dispatching plans, representing the root mean square of deviations between the actual grid-connected power of station i and the dispatching plans. The smaller this value is, the better the ability to track dispatching plans; $P_i^{\mathrm{err}}(t)$ denotes the dispatching deviation of station i in time period t; and T denotes the number of dispatching operations with a time step of 15 min, and it is set to 96.

(2) Assessment quantity indicator

$$P_i^{\mathrm{apc}}(t) = \frac{\sum_{t=1}^{T} P_i^{\mathrm{err}}(t)}{4} \tag{25}$$

where $P_i^{\mathrm{apc}}(t)$ denotes the assessment quantity indicator of station i in time period t. A smaller assessment quantity value indicates a stronger regulation capability of the energy storage system, enabling it to better fulfill dispatch instructions and thereby enhance grid stability.

(3) Energy storage utilization rate indicator

$$P_i^{\mathrm{usage}} = \frac{\sum_{k=1}^{K} \left[P_i^{\mathrm{B,c}}(k) + P_i^{\mathrm{B,d}}(k) + P_i^{\mathrm{B,up}}(k) + P_i^{\mathrm{B,down}}(k) \right]}{\sum_{k=1}^{K} P_i^{\mathrm{B,rate}}(k)} \times 100\% \tag{26}$$

where P_i^{usage} denotes the energy storage utilization rate of Station i, representing the ratio of the sum of the actual dispatch mileage of energy storage i to the sum of the frequency regulation mileage under maximum power output. The larger this value is, the higher the utilization rate of the energy storage of station i; and K denotes the number of dispatching operations with a time step of 1 min, and it is set to 1440.

V. Results and Model Validation

A. Case Study Design

To verify the effectiveness of the strategy proposed in this paper, a case study is constructed based on the generation data of a domestic wind farm and a PV power station. Among them, the dispatching plans and actual output curves of wind farm 1, wind farm 2, and the PV power station on a typical day are shown in Fig. 5, respectively. The dynamic frequency regulation signal generated with reference to the energy storage frequency regulation dispatching mechanism in the PJM market is presented in Fig. 6. The relevant parameters of the wind-storage system and the PV-storage system are listed in Table 2, and other system parameters are shown in Table 3.

To demonstrate and compare the effectiveness of the coordinated optimal dispatching strategy for the multi-wind-PV-storage system proposed in this paper, the operation and revenue of wind-storage system and PV-storage system in four scenarios are discussed respectively. Scenario 1: no energy storage; scenario 2: energy storage within the station only assists units in tracking dispatching plans without participating in frequency regulation auxiliary services; scenario 3: energy storage system at each station assists the generating unit in tracking dispatching plans and, under the existing market-based participation mode, independently participates in the frequency regulation ancillary service market as an individual market entity; and scenario 4: energy storage system at each station assists in tracking dispatching plans and participates in the frequency regulation ancillary service market through an alliance-based aggregation mode.

B. Calculation Results and Analysis

B.1 Effectiveness Analysis of Energy Storage Assisting Units in Tracking Dispatching Plans

The effectiveness of energy storage assisting units in tracking dispatching plans for all stations under different scenarios is shown in Fig. 7, and Table 4 compares the performance indicators of all stations in tracking dispatching plans under different scenarios.

As can be seen from Fig. 7, wind-storage system 1 can respond to dispatching plans in all periods except for dispatch deviations occurring in periods 92–96 (scenario 2), 93–96 (scenario 3), and 58–67, 93, and 95–96 (scenario 4), respectively. Wind-storage system 2 can respond to dispatching plans in all periods except for dispatch deviations occurring in

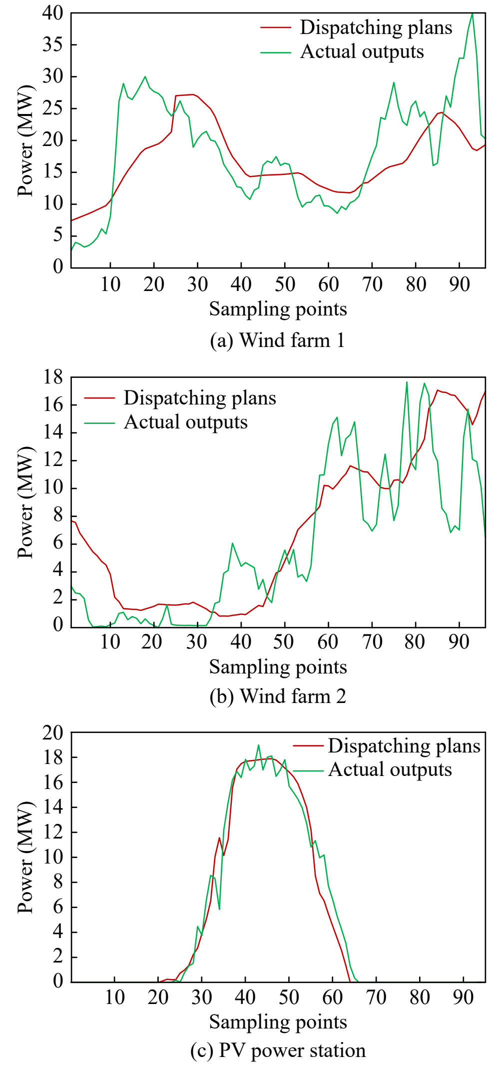

Fig. 5. Dispatching plans and actual outputs of all stations.

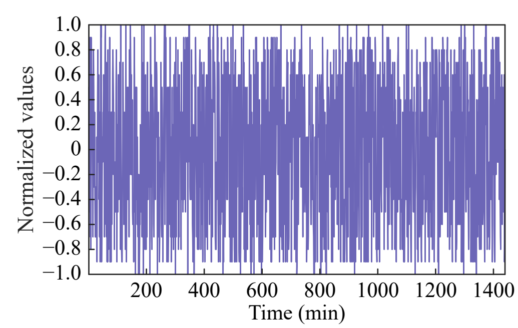

Fig. 6. Dynamic frequency regulation signals.

periods 7–32 and 85–96 under scenarios 2, 3, and 4. PV-storage system can respond to dispatching plans throughout the entire period under Scenarios 2 and 3, with a dispatch deviation occurring only in periods 35, 48, 53, and 55 in scenario 4. The reason for the different dispatch deviation periods of the stations under different scenarios is that the energy storage in

TABLE 2
RELEVANT PARAMETERS OF WIND-STORAGE SYSTEM AND PV-STORAGE SYSTEM

Project	Parameter		
	Wind farm 1	Wind farm 2	PV power station
Installed capacity of the station (MW)	88	50	20
Rated power of energy storage (MW)	20	10	5
Rated capacity of energy storage (MWh)	40	20	10
Investment cost of the energy storage (yuan)	57,000,000	44,000,000	17,400,000
Rated cycle life at 100% DoD	2500	2500	3000

TABLE 3
OTHER SYSTEM PARAMETERS

Project	Parameter
λ (yuan/MWh)	480
B^{C} (yuan/MW)	60
B^{M} (yuan/MW)	10
b	1.5
β (MWh/MW)	0.13
θ (%)	3
SOC_{min}	0.1
SOC_{max}	0.9
η^{c}, η^{d}	0.9

the stations under scenarios 2 and 3 is almost only used to assist units in tracking dispatching plans, while in scenario 4, in addition to assisting units in tracking dispatching plans, the energy storage also participates in frequency regulation auxiliary services multiple times, resulting in more charging and discharging opportunities, which is conducive to the recovery of the energy storage SOC. As shown in Fig. 7, the energy storage of wind-storage system 2 was completely unable to respond to dispatching plans during periods 7–32 under scenarios 2 and 3, but in scenario 4, due to the supplementary power obtained from participating in frequency regulation, the energy storage can intermittently respond to dispatching plans.

Further comparison of Table 4 shows that the maximum absolute value of output deviation of wind-storage system 1 is the smallest in scenario 4 and the largest in scenarios 1 and 2; the maximum absolute value of output deviation of wind-storage system 2 is the same across all scenarios, at 10.02 MW;

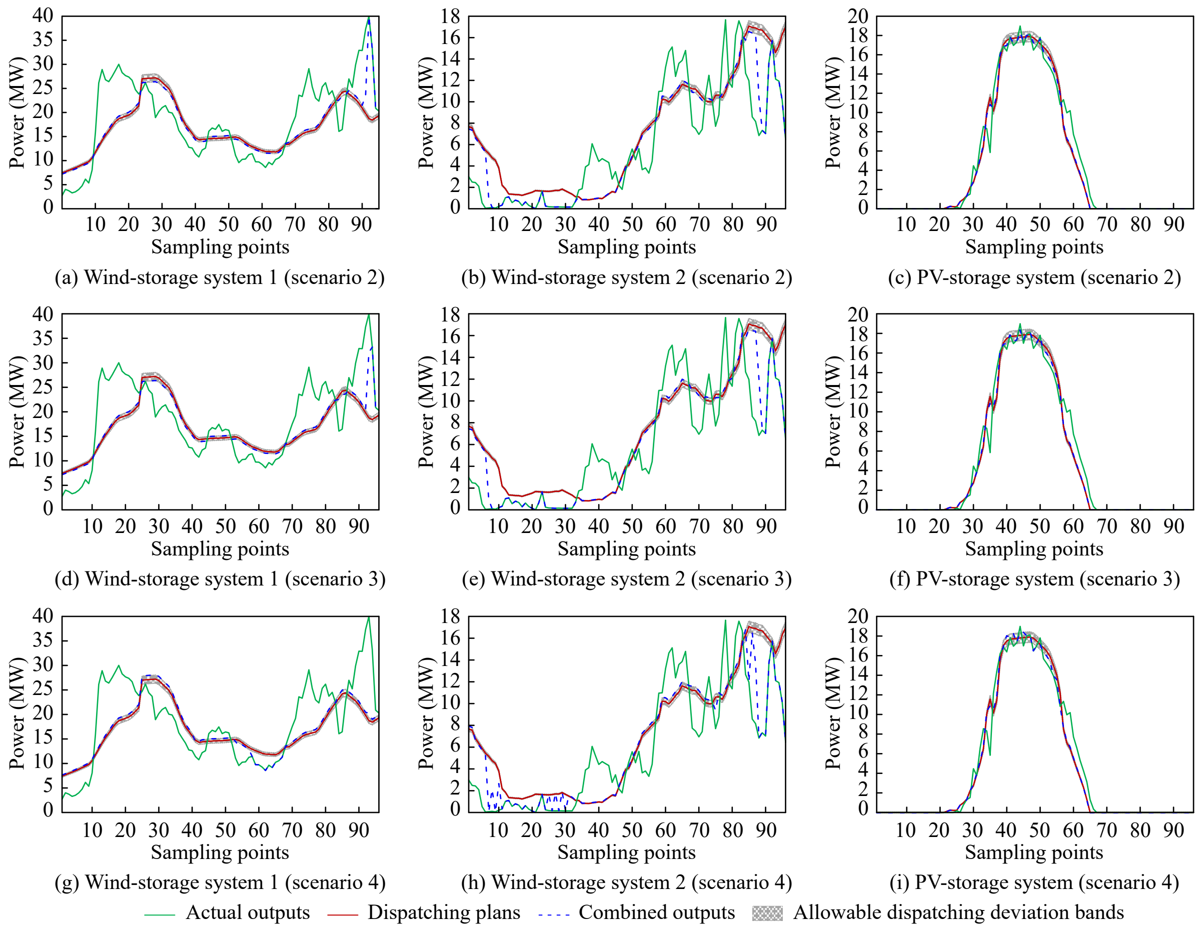

Fig. 7. Performance of all stations in tracking dispatching plans under different scenarios.

TABLE 4
PERFORMANCE INDICATORS OF ALL STATIONS IN TRACKING DISPATCHING PLANS UNDER DIFFERENT SCENARIOS

Scenario/system		Maximum absolute value of output deviation (MW)	Assessment quantity (MWh)	Indicators in tracking dispatching plans
1	Wind farm 1	20.70	112.38	0.46
	Wind farm 2	10.02	63.34	0.26
	PV power station	5.38	11.27	0.05
2	Wind-storage system 1	20.70	9.99	0.04
	Wind-storage system 2	10.02	21.66	0.09
	PV-storage system	0.38	0.10	0
3	Wind-storage system 1	14.25	7.23	0.02
	Wind-storage system 2	10.02	21.25	0.02
	PV-storage system	0.38	0.10	0
4	Wind-storage system 1	2.99	5.00	0.02
	Wind-storage system 2	10.02	23.18	0.09
	PV-storage system	1.02	0.91	0

and the maximum absolute value of output deviation of PV-storage system is the smallest in scenarios 2 and 3 and the largest in scenario 1. The assessment electricity quantity of wind-storage system 1 is the smallest in scenario 4; that of wind-storage system 2 is the smallest in scenario 3; and that of PV-storage system is relatively small in both scenarios 2 and 3, at 0.10 MWh. By comparing the dispatching plan tracking indicators between scenarios 2 and 4, it can be found that the P^{index} indicator of wind-storage system 1 in scenario 4 is 50% lower than that in scenario 2, while the P^{index} indicators of wind-storage system 2 and PV-storage system are the same in both scenarios 2 and 4. Therefore, the strategy proposed in this paper can improve the ability of energy storage in stations to assist units in tracking dispatching plans.

B.2 Analysis of Energy Storage Participation in the Frequency Regulation Auxiliary Service Market

The frequency regulation capacity declared by all stations to the energy storage alliance agent under scenario 4 is shown in Fig. 8, and the winning capacity after the integrated calculation of the declared frequency regulation capacity by all stations in each period by the energy storage alliance agent is shown in Fig. 9.

As can be seen from Fig. 8, since wind farms operate continuously 24 h a day, the station's energy storage needs to determine whether it is necessary to assist the unit in tracking the dispatching plan during each dispatching period. The remaining power of the station's energy storage often only has a unidirectional output capacity, so the declared frequency regulation capacity of wind-storage system 1 and wind-storage system 2 is mostly either upward or downward frequency regulation capacity in each period. In addition, wind-storage system 1 and wind-storage system 2 declared bidirectional frequency regulation capacity in period 83 and periods 57, 67, 74, and 79, respectively, because the actual output of the wind farm was within the allowable deviation range of the dispatching plan during these periods. In contrast, affected by its power

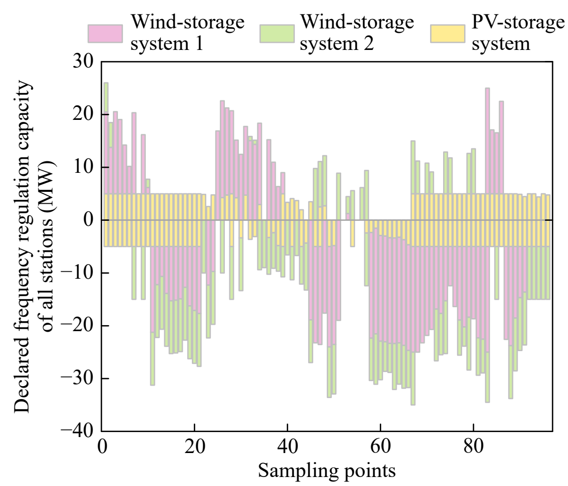

Fig. 8. Declared frequency regulation capacity of all stations.

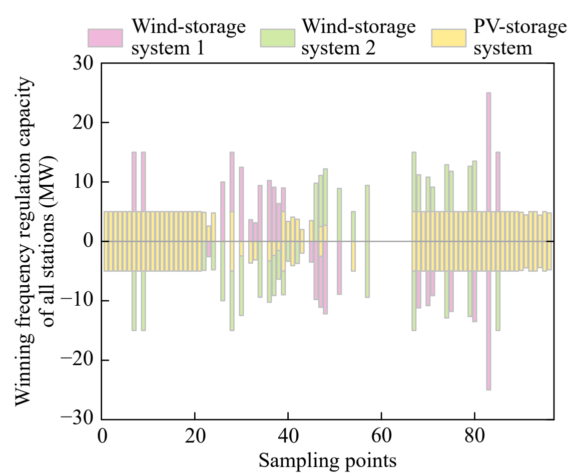

Fig. 9. Winning frequency regulation capacity of all stations.

generation characteristics, PV-storage system only generates power during the day. Therefore, it declared bidirectional frequency regulation capacity in both periods 1–21 and 67–96, and only declared unidirectional frequency regulation capacity in other periods because it needed to assist the unit in tracking the dispatching plan.

As can be seen from Fig. 9, since the declared frequency regulation capacity of PV-storage system in periods 1–21 and 67–96 includes equivalent upward and downward frequency regulation capacity, all the declared frequency regulation capacity of PV-storage system was awarded in these periods. In addition, to meet the access requirements of the frequency regulation auxiliary service market, the energy storage alliance agent integrated the unidirectional frequency regulation capacity declared by each station with the goal of maximizing the declared frequency regulation capacity in each period. Taking period 48 in Fig. 9 as an example, the upward frequency regulation capacity in this period consists of wind-storage system 2 and PV-storage system, with the two stations awarded 9.48 and 1.29 MW, respectively, while the downward frequency regulation capacity is composed of wind-storage system 1, with the station awarded 10.77 MW. The participation mode of the energy storage alliance in the frequency regulation auxiliary service market can provide more opportunities for stations to participate in frequency regulation auxiliary services, thus increasing the revenue of stations from participating in auxiliary services.

The composition of energy storage output and the SOC variation curves of energy storage for all stations under different scenarios are shown in Figs. 10 and 11, respectively. As shown in Fig. 10, in scenario 2, the energy storage in stations only assists units in tracking dispatching plans, so the energy storage output of each station consists solely of power for assisting dispatching plans. In scenario 3, the energy storage in stations participates in frequency regulation auxiliary services independently when meeting the frequency regulation market access requirements, the energy storage output composition of wind-storage system 1 and wind-storage system 2 includes a small amount of frequency regulation response power, while the energy storage output of PV-storage system is mainly composed of frequency regulation response power. The reason is that wind farms generate power continuously throughout the day, and deviations between the actual output and the dispatch plan exist during most periods. As a result, the energy storage system must give priority to assisting the generating unit in tracking the dispatch plan, leaving relatively limited remaining power available for frequency regulation. In contrast, PV plants generate power only during daytime, and during nighttime as well as some non-generating periods, energy storage is not required to continuously correct dispatch plan

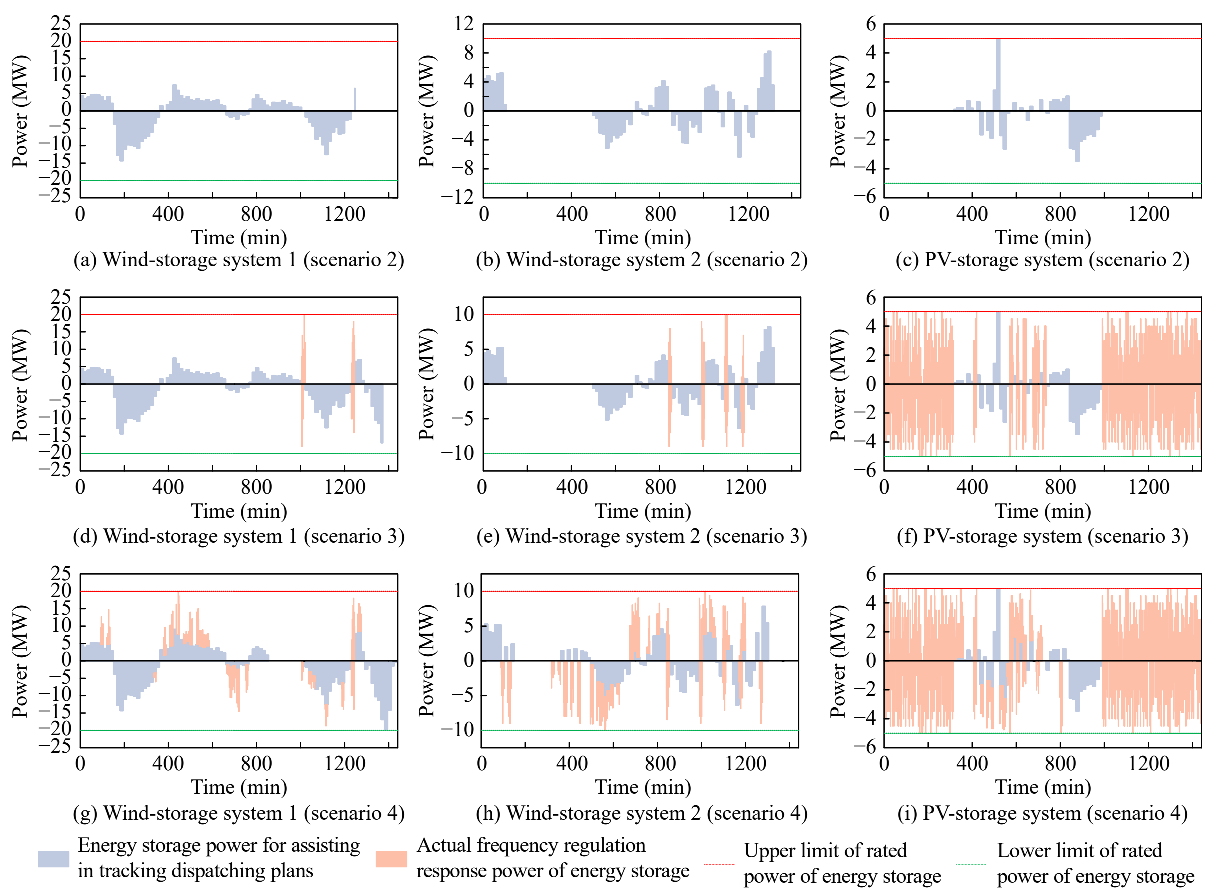

Fig. 10. Composition of energy storage output of all stations under different scenarios.

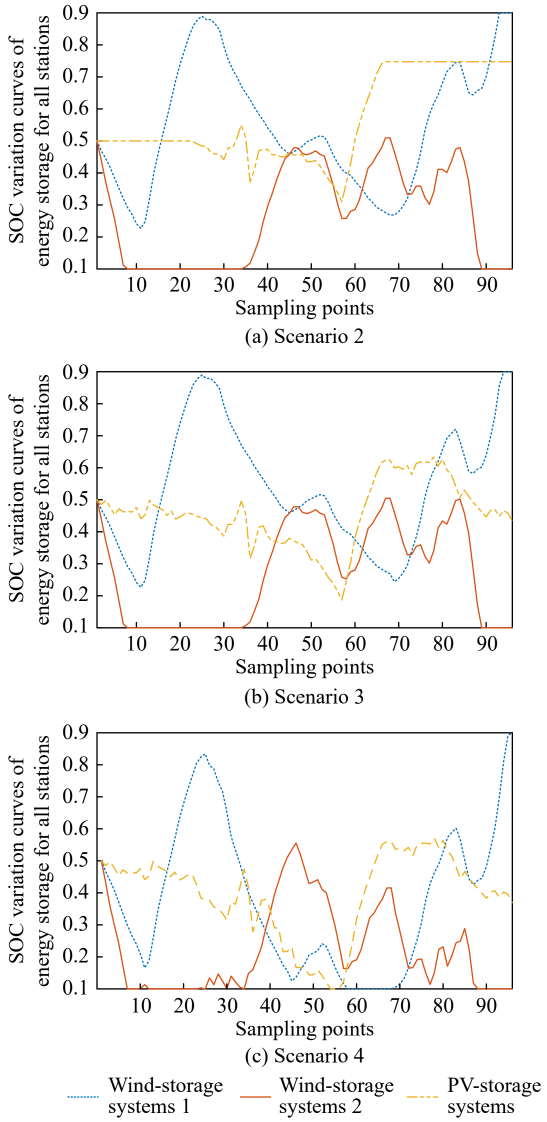

Fig. 11. SOC variation curves of energy storage for all stations under different scenarios.

deviations. Therefore, the storage system has more remaining regulation capability available for frequency regulation services. Compared with scenario 3, in scenario 4 where stations participate in the frequency regulation auxiliary service market through the energy storage alliance, the unidirectional remaining regulation capacities of wind-storage system 1 and wind-storage system 2 can be integrated through the alliance and converted into effective awarded capacity; therefore, the proportion of frequency regulation response power in the storage output of both systems increases significantly. As shown in Fig. 11, due to the similar composition of energy storage output, the SOC variation of energy storage for all stations in scenarios 2 and 3 is basically consistent. In scenario 4, due to the substantial frequency regulation output of station energy storage, the SOC maintenance effect of energy storage in wind-storage system 1 and PV-storage system is slightly worse than that in scenarios 2 and 3.

To further analyze the participation of energy storage in the frequency regulation auxiliary service market, the utilization rate indicators of energy storage for all stations under different scenarios are calculated, and the results are shown in Table 5. Compared with that in scenario 2, the energy storage utilization rate of wind-storage system 1 in scenario 4 increased by 5.57%, that of wind-storage system 2 increased by 5.46%, and that of PV-storage system increased by 31.57%. Under the strategy proposed in this paper, the application scenarios of station energy storage have shifted from a single scenario of assisting units in tracking dispatching plans to multiple scenarios where they can simultaneously participate in frequency regulation auxiliary services. This can effectively improve the utilization rate of energy storage in RPP and shorten the investment payback period of energy storage.

B.3 Economic Analysis of Stations

Table 6 presents the abandoned wind and PV power of all stations under different scenarios.

As can be seen from Table 6, the abandoned wind power of wind-storage system 1 in scenario 4 is less than that in scenarios 2 and 3. After configuring energy storage, the abandoned wind and PV power of wind farm 2 and PV power station have been reduced to 0 MWh.

Tables 7–9 present the operating costs, revenues, and profits of each station in scenarios 2–4, respectively. As can be seen from Table 9, the total profit of wind-storage system 1 in scenario 4 is 187,484.54 yuan, an increase of 4.96% compared with that in scenario 3, among which the frequency regulation revenue has increased by 113.13%. The total profit of wind-storage system 2 in scenario 4 is 51,734.99 yuan, an increase of 10.49% compared with that in scenario 3, with the frequency regulation revenue increasing by 107.89%. As can be seen from Table 8, this is mainly because, under scenario 4,

TABLE 5
UTILIZATION RATE OF ENERGY STORAGE FOR ALL STATIONS UNDER DIFFERENT SCENARIOS

Scenario	Energy storage utilization rate indicator P_i^{usage} (%)		
	Wind-storage system 1	Wind-storage system 2	PV-Storage system
2	21.33	17.37	9.31
3	22.96	19.70	40.43
4	26.90	22.83	40.88

TABLE 6
ABANDONED WIND AND PV POWER OF ALL STATIONS UNDER DIFFERENT SCENARIOS

Scenario	Abandoned wind and PV power (MWh)		
	Wind-storage system 1	Wind-storage system 2	PV-storage system
1	74.51	19.05	7.40
2	9.99	0	0
3	7.23	0	0
4	0.28	0	0

TABLE 7
OPERATING COSTS OF ALL STATIONS UNDER DIFFERENT SCENARIOS

Scenario/system		Lifetime loss cost (yuan)	Energy loss cost (yuan)	Output deviation penalty cost (yuan)
2	Wind-storage system 1	10,839.65	5116.75	9587.17
	Wind-storage system 2	8249.42	2121.28	20,792.98
	PV-storage system	1336.14	1115.41	92.35
3	Wind-storage system 1	11,482.78	5510.82	6943.02
	Wind-storage system 2	8457.46	2404.00	20,398.42
	PV-storage system	2080.69	2446.16	92.35
4	Wind-storage system 1	15,158.55	6465.13	4796.57
	Wind-storage system 2	10,052.14	2780.47	22,248.18
	PV-storage system	2528.13	2475.00	870.24

TABLE 8
OPERATING REVENUES OF ALL STATIONS UNDER DIFFERENT SCENARIOS

Scenario/system		Energy revenue (yuan)	Frequency regulation revenue (yuan)
2	Wind-storage system 1	19,4691.19	0
	Wind-storage system 2	69,869.00	0
	PV-storage system	50,573.82	0
3	Wind-storage system 1	19,4691.19	7872.00
	Wind-storage system 2	70,066.28	8016.00
	PV-storage system	50,573.82	57,729.00
4	Wind-storage system 1	197,127.17	16,777.62
	Wind-storage system 2	70,151.59	16,664.19
	PV-storage system	50,637.36	57,567.01

TABLE 9
OPERATING PROFIT OF ALL STATIONS UNDER DIFFERENT SCENARIOS

Scenario/system		Total cost (yuan)	Total revenue (yuan)	Total profit (yuan)
2	Wind-storage system 1	25,543.57	194,691.19	16,9147.62
	Wind-storage system 2	31,163.68	69,869.00	38,705.32
	PV-storage system	2543.9	50,573.82	48,029.92
3	Wind-storage system 1	23,936.62	202,563.19	178,626.57
	Wind-storage system 2	31,259.88	78,082.28	46,822.4
	PV-storage system	4619.2	108,302.82	103,683.62
4	Wind-storage system 1	26,420.25	213,904.79	187,484.54
	Wind-storage system 2	35,080.79	86,815.78	51,734.99
	PV-storage system	5873.37	108,204.37	102,331

the energy storage alliance effectively integrates the unidirectional remaining regulation capability of each station, enabling the wind-storage systems to gain more opportunities to participate in frequency regulation ancillary services, thereby increasing their frequency regulation revenue and significantly improving their total profit. The total profit of PV-storage system in scenario 4 is 102,331 yuan, slightly lower than that in scenario 3. The main reason is that, under scenario 3, the PV-storage station is already able to participate in the frequency regulation market independently by virtue of its strong bidirectional frequency regulation capability. Therefore, under scenario 4, the incremental revenue brought by the alliance-based participation mode is relatively limited, and the additional revenue is basically offset by the additional costs, resulting in a slight decrease in the total profit.

C. Verification of strategy stability under high Wind- or PV variability scenarios

In practical engineering scenarios, wind and PV generation is subject to significant uncertainty, which can lead to larger deviations between actual and scheduled outputs. To better reflect real-world conditions, this subsection amplifies the fluctuation magnitude of the actual wind-PV output relative to the dispatching plan, and compares the corresponding performance indices against those under the original wind-PV profiles, so as to verify the stability of the proposed strategy under high wind-PV variability.

The high-variability scenario adopted in this paper is constructed as follows for the units' actual power output

$$P_i^{\mathrm{W,high}}(t) = P_i^{\mathrm{WP}}(t) + \alpha(P_i^{\mathrm{W}}(t) - P_i^{\mathrm{WP}}(t)) \qquad (27)$$

where $P_i^{\mathrm{W,high}}(t)$ denotes the actual power output of station i in time period t; and α denotes deviation coefficient of actual output relative to the dispatching plan, and it is set to 1.2.

The tracking performance of the storage-assisted units at each station under the high-variability scenario is illustrated in Fig. 12. Table 10 compares the dispatch-tracking performance indices of each station under two scenarios.

Compared with the original scenario, wind-storage system 1 exhibits additional dispatch deviations at time intervals 23, 44, 54, 57, and 92, while it follows the dispatch schedule in the remaining intervals. Wind-storage system 2 does not show an increase in the number of intervals with dispatch deviations; however, when deviations occur, their magnitudes are farther away from the deviation band, whereas the other intervals largely coincide with those in the original scenario. The PV-storage plant shows one fewer dispatch deviation at interval 48 but additional deviations at intervals 51, 52, and 54, and it follows the dispatch schedule in all other intervals.

Scenario 5 denotes the high-variability scenario.

D. Analysis of the economic impacts of frequency regulation mileage price variations

This subsection considers different frequency regulation mileage prices and analyzes how changes in the mileage price affect plant-level utilization and revenues.

In the preceding subsections, the regulation mileage price is set to 10, which is regarded as the baseline market incentive.

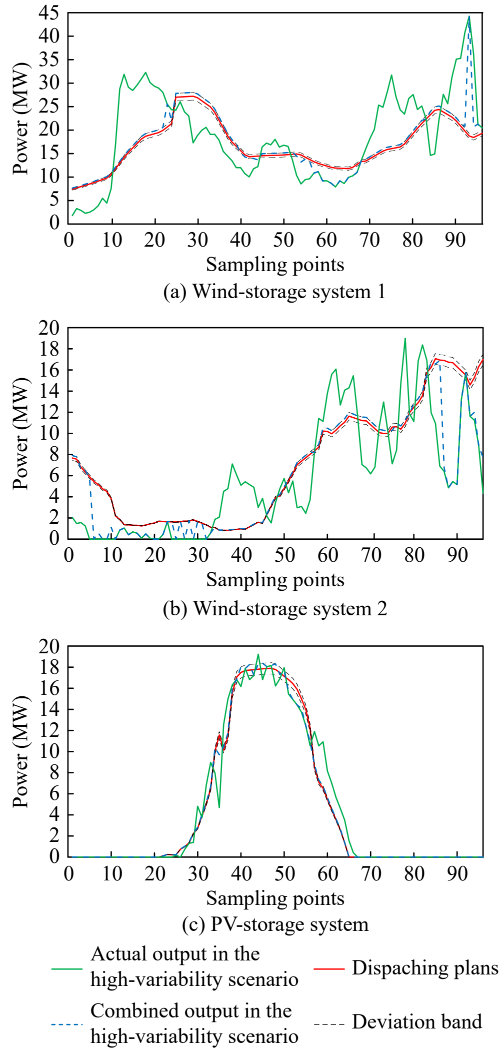

Fig. 12. Performance of all stations in tracking dispatching plans under two scenarios.

In what follows, the variation trends of the relevant indices are analyzed under a low-incentive market regime ($B^{\mathrm{M}}=5$) and a high-incentive market regime ($B^{\mathrm{M}}=20$).

TABLE 10
PERFORMANCE INDICATORS OF ALL STATIONS IN TRACKING DISPATCHING PLANS UNDER TWO SCENARIOS

Scenario/system		Maximum absolute value of output deviation (MW)	Assessment quantity (MWh)	Indicators in tracking dispatching plans
	Wind-storage system 1	2.99	5.00	0.02
4	Wind-storage system 2	10.02	23.18	0.09
	PV-storage system	1.02	0.91	0
	Wind-storage system 1	24.95	16.29	0.07
5	Wind-storage system 2	11.39	27.53	0.11
	PV-storage system	1.53	1.57	0.01

It can be observed from the operation that changes in the frequency regulation mileage price do not alter the number of energy storage actions, and therefore, the energy storage utilization rate remains unchanged.

As can be seen from Table 11, as the regulation mileage price increases, the total cost remain unchanged, while the increase in frequency regulation mileage leads to higher frequency regulation revenue, which in turn improves the total profit of the station.

E. Ultra-short-term Forecast Error Sensitivity Analysis

To examine the sensitivity of the rolling optimization results to ultra-short-term forecast errors, some forecast error scenarios are constructed on the basis of the benchmark case. Let the ultra-short-term forecast output of station i in time period t be defined as

$$P_i^{\mathrm{ST}}(t)=(1+\varepsilon_i)P_i^{\mathrm{WB}}(t) \tag{28}$$

where $P_i^{\mathrm{ST}}(t)$ denotes the ultra-short-term forecast output of station i in time period t, and ε_i denotes the forecast error coefficient.

To more intuitively reflect the sensitivity of the proposed strategy to ultra-short-term forecast errors under different error scenarios, the three systems are aggregated. A comparative analysis is then conducted on the changing trends of total

TABLE 11
OPERATING PROFIT OF ALL STATIONS UNDER DIFFERENT INCENTIVE

Incentive/system		Total cost (yuan)	Total revenue (yuan)	Total profit (yuan)
	Wind-storage system 1	26,420.25	20,8417.4	181,997.15
Low	Wind-storage system 2	35,080.79	81,282.23	46,201.44
	PV-storage system	5873.37	88,133.9	82,260.53
	Wind-storage system 1	26,420.25	213,904.79	187,484.54
Base	Wind-storage system 2	35,080.79	86,815.78	51,734.99
	PV-storage system	5873.37	108,204.37	102,331
	Wind-storage system 1	26,420.25	224,879.57	198,459.32
High	Wind-storage system 2	35,080.79	97,882.88	62,802.09
	PV-storage system	5873.37	148,345.3	142,471.93

assessment quantity and total profit under different error scenarios, as shown in Table 12.

TABLE 12
VARIATION OF EACH INDICATOR UNDER DIFFERENT ERROR SCENARIOS

Scenario	Total assessment quantity (MWh)	Total profit (yuan)
3	28.58	329,133
4	29.09	341,551
1% error	27.72	346,930
2% error	27.63	350,420
3% error	27.43	347,310
4% error	27.87	349,530
5% error	32.74	346,460
6% error	35.67	341,820
7% error	41.69	335,330
8% error	52.94	315,040

The results show that when the value of ε_i lies within a certain point between 4% and 5%, the total assessment quantity begins to exceed that of the benchmark strategy; when it lies within a certain point between 7% and 8%, the total profit begins to fall below that of the benchmark strategy. This indicates that the proposed strategy still maintains advantages in tracking dispatch performance and economic performance within a certain range of ultra-short-term forecast errors, demonstrating good adaptability to such forecast errors within that range.

F. Case study analysis considering stochastic MPC and chance-constrained methods

To further enhance the robustness of the proposed rolling optimization dispatch method under renewable energy forecast errors, this paper introduces an SMPC approach based on the original rolling optimization framework, considering the impact of ultra-short-term forecast uncertainty on dispatch decisions. During the rolling optimization process, the actual output can be expressed as

$$P_i^{\mathrm{act}}(t) = P_i^{\mathrm{ST}}(t) + \xi_t \tag{29}$$

where $P_i^{\mathrm{act}}(t)$ denotes the actual output of station i in time period t, and ξ_t denotes the forecast error random variable.

This paper assumes that the ultra-short-term forecast errors of wind power and PV follow a normal distribution with a mean of zero.

$$\begin{aligned} &\xi_t \sim N(0, \sigma_t^2) \\ &\sigma_t = \rho P_i^{\mathrm{ST}}(t) \end{aligned} \tag{30}$$

where σ_t denotes the standard deviation of the forecast error, and ρ denotes the forecast error scaling coefficient. In this paper, the value is set to 8% for wind power stations and 10% for PV stations.

The equivalent output considering forecast errors is given by

$$P_i^{\mathrm{net}}(t) = P_i^{\mathrm{ST}}(t) + P_i^{\mathrm{B,d}}(t) - P_i^{\mathrm{B,c}}(t) \tag{31}$$

To ensure the reliability of energy storage-assisted tracking of the dispatch plan, this paper further introduces a chance-constrained method, extending the plan-tracking constraints from deterministic constraints to probabilistic constraints.

$$\begin{aligned} &\Pr(P_i^{\mathrm{net}}(t) \leqslant P_i^{\mathrm{WP,up}}(t)) \geqslant 1-\varepsilon \\ &\Pr(P_i^{\mathrm{net}}(t) \geqslant P_i^{\mathrm{WP,down}}(t)) \geqslant 1-\varepsilon \end{aligned} \tag{32}$$

where $\Pr(\cdot)$ denotes the probability operator, and it is used to characterize the probability level that the constraints are satisfied under the influence of the forecast error random variable; and ε denotes the violation probability, and the value is set to 5%.

Under the assumption that the forecast error follows a normal distribution, the above probabilistic constraint can be transformed into an equivalent deterministic form.

$$\begin{aligned} &P_i^{\mathrm{ST}}(t) + P_i^{\mathrm{B}}(t) + z_\varepsilon \sigma_t \leqslant P_i^{\mathrm{WP,up}}(t) \\ &P_i^{\mathrm{ST}}(t) + P_i^{\mathrm{B}}(t) - z_\varepsilon \sigma_t \geqslant P_i^{\mathrm{WP,down}}(t) \end{aligned} \tag{33}$$

Since the above model requires relatively strict parameter selection, this paper further adopts a soft chance-constrained formulation.

$$\begin{aligned} &P_i^{\mathrm{ST}}(t) + P_i^{\mathrm{B}}(t) + z_\varepsilon \sigma_t \leqslant P_i^{\mathrm{WP,up}}(t) + s_t \\ &P_i^{\mathrm{ST}}(t) + P_i^{\mathrm{B}}(t) - z_\varepsilon \sigma_t \geqslant P_i^{\mathrm{WP,down}}(t) - s_t \\ &s_t \geqslant 0 \end{aligned} \tag{34}$$

where z_ε denotes the quantile of the standard normal distribution and s_t denotes the slack variable.

Under the SMPC and chance-constrained model that considers forecast uncertainty, simulation analyses were conducted for three renewable power stations. The results of the tracking performance indicators, compared with those of the original method, are shown in Table 13.

By comparing the tracking performance indicators of the two methods, it can be observed that different types of renewable energy systems exhibit significantly different behaviors after incorporating forecast uncertainty. For wind-storage system 1, the tracking performance index increases from 0.02 to 0.05. This indicates that, after considering forecast errors, the dispatch strategy of wind-storage system 1 becomes more conservative, as the energy storage system needs to reserve regulation margins, leading to reduced tracking accuracy in some periods. For wind-storage system 2, the tracking performance index decreases from 0.09 to 0.08. This suggests that for wind farms with larger fluctuations, the stochastic MPC method can effectively reduce the accumulation of deviations caused by forecast errors, thereby significantly improving tracking per-

TABLE 13
PERFORMANCE INDICATORS OF ALL STATIONS IN TRACKING DISPATCHING PLANS UNDER TWO METHODS

Method/system		Maximum absolute value of output deviation (MW)	Assessment quantity (MWh)	Indicators in tracking dispatching plans
MPC	Wind-storage system 1	2.99	5.00	0.02
	Wind-storage system 2	10.02	23.18	0.09
	PV-storage system	1.02	0.91	0
SMPC	Wind-storage system 1	14.48	12.37	0.05
	Wind-storage system 2	9.40	18.86	0.08
	PV-storage system	0.38	0.10	0

formance. For the PV-storage system, the maximum deviation decreases from 1.02 to 0.38 MW, and the assessment quantity decreases from 0.91 to 0.10 MWh, indicating that the PV system achieves near-perfect tracking under the stochastic MPC method, with the impact of forecast errors being effectively suppressed.

The SOC variation curves of each station before and after incorporating forecast uncertainty are shown in Fig. 13.

As can be observed from Fig. 13, after introducing SMPC, the SOC variation range of each system increases overall, and in some periods it even approaches the upper and lower SOC bounds more frequently. The main reasons are as follows: In deterministic MPC, the rolling optimization is based only on a single forecast trajectory, and the charging/discharging behavior of energy storage mainly serves as a passive correction of current deviations. In contrast, in SMPC, the optimization model considers forecast error scenarios and their probability distributions, requiring the energy storage system to reserve regulation capacity for future uncertainties. As a result, the storage system may charge or discharge in advance during certain periods, leading to more pronounced dynamic fluctuations in the SOC trajectory. In addition, since wind power typically exhibits higher randomness and volatility than PV, its forecast error distribution is generally wider. Under the influence of chance constraints, the wind-storage systems need to adjust their storage states more frequently, resulting in more pronounced SOC fluctuations compared with PV-storage systems.

To further analyze the utilization of energy storage at each station after introducing SMPC, a comparative analysis of the energy storage utilization rate before and after the modification is conducted, as shown in Table 14.

From the energy storage utilization results, it can be observed that under the improved method, the utilization rates of wind-storage system 1 and wind-storage system 2 increase from 26.90% and 22.83% to 28.72% and 27.07%, respectively, while the utilization rate of the PV-storage system decreases from 40.88% to 18.99%. This indicates that, after considering forecast uncertainty, the utilization patterns of

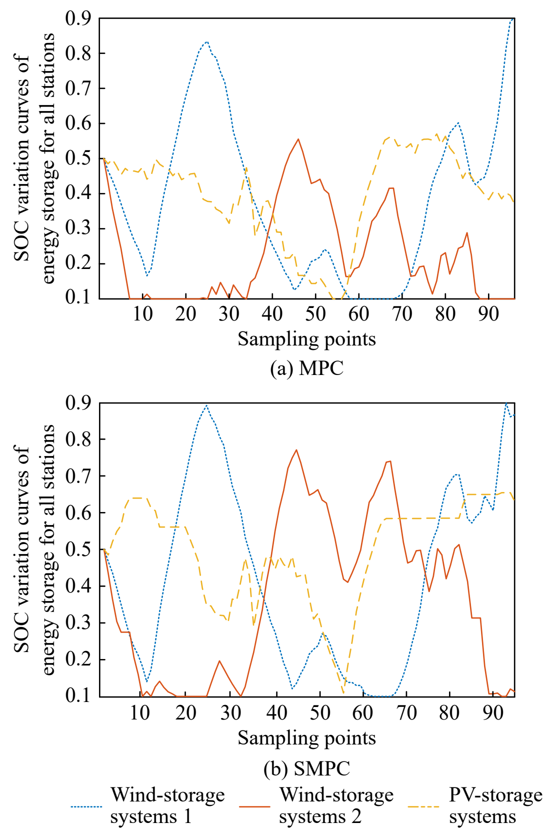

Fig. 13. SOC variation curves of energy storage for all stations under two methods.

TABLE 14
UTILIZATION RATE OF ENERGY STORAGE FOR ALL STATIONS UNDER TWO METHODS

Method	Energy storage utilization rate indicator P_i^{usage} (%)		
	Wind-storage system 1	Wind-storage system 2	PV-storage system
MPC	26.90	22.83	40.88
SMPC	28.72	27.07	18.99

energy storage in different types of renewable power stations exhibit clear differentiation.

An economic analysis of the renewable power stations is conducted, as shown in Table 15.

TABLE 15
OPERATING PROFIT OF ALL STATIONS UNDER TWO METHODS

Method/system		Total cost (yuan)	Total revenue (yuan)	Total profit (yuan)
MPC	Wind-storage system 1	26,420.25	208,417.4	181,997.15
	Wind-storage system 2	35,080.79	81,282.23	46,201.44
	PV-storage system	5873.37	88,133.9	82,260.53
SMPC	Wind-storage system 1	35,504.4	223,930.94	188,426.55
	Wind-storage system 2	34,412.89	95,424.69	61,011.8
	PV-storage system	4045.75	64,445.71	60,399.96

The total profit of wind-storage system 1 increases slightly from 187,484.54 to 188,426.55 yuan; the total profit of wind-storage system 2 increases from 51,734.99 to 61,011.80 yuan, representing a 17.9% improvement; while the total profit of the PV-storage station decreases significantly from 102,331 to 60,399.96 yuan. These results indicate that the stochastic MPC approach is more suitable for application in wind-storage systems with high volatility scenarios.

VI. CONCLUSIONS

To improve the dispatching plan tracking capability, energy storage utilization rate, and revenue of RPP with energy storage, as well as ensure the safe and stable operation of the power grid, a coordinated optimal dispatch strategy for multi wind-PV-storage system considering energy storage-assisted dispatching plan tracking and frequency regulation participation is proposed. Simulation verification is conducted, and the following conclusions are drawn:

(1) The optimal energy storage control strategy proposed in this paper can enhance the capability of station energy storage to assist units in tracking dispatching plans. Compared with the scenario without energy storage, the dispatching tracking performance indicators of wind-storage system 1, wind-storage system 2, and PV-storage system are reduced by 95.65%, 65.38%, and 100%, respectively.

(2) The strategy of energy storage alliance participating in the frequency regulation auxiliary service market proposed in this paper transforms the application scenario of station energy storage from a single dispatching plan assistance to a multi-scenario that combines dispatching plan assistance with frequency regulation auxiliary service participation. This can effectively improve the energy storage utilization rate of RPP. Compared with the scenario where energy storage only assists in dispatching plan tracking, the energy storage utilization rates of wind-storage system 1, wind-storage system 2, and PV-storage system are increased by 5.57%, 5.46%, and 31.57%, respectively.

(3) Under the strategy proposed in this paper, the total profits of wind-storage system 1 and wind-storage system 2 are increased by 4.96% and 10.49%, respectively, compared with the scenario where energy storage assists in dispatching plan tracking and participates in frequency regulation auxiliary services independently. This effectively improves the economic benefits of RPP.

(4) The proposed strategy in this paper demonstrates good scenario adaptability, making it suitable for high wind-PV variability scenarios and capable of effectively adapting to market incentive fluctuations.

DECLARATION OF COMPETING INTEREST

The authors declare that they have no known competing financial interests or personal relationships that could have appeared to influence the work reported in this paper.

FUNDING

This work was supported by Key Projects of the National Natural Science Foundation of China under Grand No. 52337004.

AI USAGE STATEMENT

During the preparation of this work, the authors used AI-assisted tools in order to language polishing only. The authors have reviewed and edited the content and take full responsibility for the final version of the manuscript.

REFERENCES

[1] S. S. Das, J. Kumar, S. Dawn, and F. Salata, "Existing stature and possible outlook of renewable power in comprehensive electricity market," *Processes*, vol. 11, no. 6, pp. 1849, Jun. 2023.

[2] M. Khalid, "Smart grids and renewable energy systems: perspectives and grid integration challenges," *Energy Strategy Rev.*, vol. 51, pp. 101299, Jan. 2024.

[3] Y. L. Pan and F. Dong, "Dynamic evolution and driving factors of new energy development: fresh evidence from China," *Technol. Forecasting Soc. Change*, vol. 176, pp. 121475, Mar. 2022.

[4] X. X. Long, Y. Z. Li, Y. Li, L. J. G, H. B. Gooi, C. Y. Chung, and Z. G. Zeng. "Collaborative response of data center coupled with hydrogen

storage system for renewable energy absorption," *IEEE Trans. Sustain. Energy*, vol. 15, no. 2, 986–1000, Apr. 2024.

[5] Y. H. Nie, Z. Li, J. Zhang, L. Gao, Y. Li, and H. Y. Zhou. "Optimal dispatch strategy for a multi-microgrid cooperative alliance using a two-stage pricing mechanism," *IEEE Trans. Sustain. Energy*, vol. 16, no. 1, 174–188, Jan. 2025.

[6] National Energy Administration. (2025, Nov.). China's power industry statistics (January–October 2025). [Online]. Available: https://www.nea.gov.cn/20251125/c08a5f9b4a54481696a432ecd6c70dd3/c.html.

[7] J. Ren, M. Gao, S. Cheng, X. D. Zhang, and Y. B. Liu, "A balance method for power supply-demand adapting to high uncertainties of renewable energy in northwest power grid," *Electr. Power*, vol. 56, no. 9, pp. 66–78, Sep. 2023.

[8] X. W. Ma, W. Z. Wang, C. Xue, X. D. Li, P. H. Li, and X. Liu, "Research on the leading demonstration system of new-type power system in Northwest China," *Power Syst. Clean Energy*, vol. 40, no. 1, pp. 1–7, Jan. 2024.

[9] X. Zhou, Y. S. Liu, J. F. Dai, and T. F. Zhang, "Quantitative analysis of power system frequency characteristics considering wind power-energy storage-flexible HVDC transmission participation in frequency modulation," *Power Syst. Prot. Control*, vol. 51, no. 6, pp. 30–44, Mar. 2023.

[10] Y. Jiang, A. Bernstein, P. Vorobev, and E. Mallada, "Grid-forming frequency shaping control for low-inertia power systems," *IEEE Control Syst. Lett.*, vol. 5, no. 6, pp. 1988–1993, Dec. 2021.

[11] Y. M. Ruan, Q. H. Zong, W. Yao, H. Y. Zhou, X. H. Zhang, and J. Y. Wen, "Quantitative assessment and analysis of influencing factors on frequency regulation capability of wind farms considering typical control," *Autom. Electr. Power Syst.*, vol. 48, no. 8, pp. 42–52, Apr. 2024.

[12] Z. W. Li, Z. P. Cheng, J. Liang, and J. K. Si, "Distributed cooperative AGC method for new power system with heterogeneous frequency regulation resources," *IEEE Trans. Power Syst.*, vol. 38, no. 5, pp. 4928–4939, Sep. 2023.

[13] J. B. Guo, Y. R. Jing, W. L. Hou, T. Z. Wang, S. C. Ma, and G. Q. He, "Demands and challenges of energy storage technology for future power system," *Energy Internet*, vol. 1, no. 2, pp. 116–122, Nov. 2024.

[14] T. Zhang and Y. N. Wu, "Collaborative allocation model and balanced interaction strategy of multi flexible resources in the new power system based on Stackelberg game theory," *Renewable Energy*, vol. 220, pp. 119714, Jan. 2024.

[15] S. Kuang and B. B. Wang, "Optimization strategy of wind storage joint operation considering energy storage life and participating in frequency modulation service," *Power Gener. Technol.*, vol. 41, no. 1, pp. 73–78, Feb. 2020.

[16] J. Y. Zhou, "Optimization of the fast frequency regulation strategy for energy storage-assisted photovoltaic power stations," *Distrib. Gener. Altern. Energy J.*, vol. 39, no. 2, pp. 263–296, Feb. 2024.

[17] W. L. Fu, Q. A. Zhuo, Y. C. Wu, N. Fang, H. R. Zhang, and X. Chen, "Distributed robust planning for energy storage capacity with multi-energy complementarity providing frequency support," *Power Syst. Technol.*, vol. 48, no. 1, pp. 282–290, Jan. 2024.

[18] T. X. Yang, Y. H. Huang, J. R. Tang, D. Wang, K. L. Zhou, and G. R. Zhu, "Multi-objective optimization of energy storage system with frequency regulation control under high proportion of renewable energy," *High Voltage Eng.*, vol. 49, no. 7, pp. 2744–2753, Jul. 2023.

[19] M. B. Abdelghany, V. Mariani, D. Liuzza, and L. Glielmo, "Hierarchical model predictive control for islanded and grid-connected microgrids with wind generation and hydrogen energy storage systems," *Int. J. Hydrogen Energy*, vol. 51, pp. 595–610, Jan. 2024.

[20] C. Qian, N. He, Z. H. Cheng, R. X. Li, and L. Yang, "Double-layer optimal scheduling method for solar photovoltaic thermal system based on event-triggered MPC considering battery performance degradation," *Energy*, vol. 304, pp. 132233, Sep. 2024.

[21] L. Yang, S. N. Li, W. Huang, D. Zhang, H. S. Ma, S. D. Xu, B. Yang, and X. S. Zhang, "Optimal coordinated control of multi-source for AGC with participation of wind and solar energy," *Power Syst. Prot. Control*, vol. 48, no. 19, pp. 43–49, Oct. 2020.

[22] J. H. Li, T. Hou, G. G. Yan, C. P. Li, and G. Mu, "Two-layer optimization of frequency modulation power in multi-battery energy storage system considering frequency modulation cost and recovery of state of charge," *Proc. CSEE*, vol. 41, no. 23, pp. 8020–8032, Dec. 2021.

[23] S. Q. Zhang, B. Yuan, Z. D. Ji, X. J. Wei, and J. F. Zhao, "A secondary frequency control based on the distributed control theory considering battery energy storage systems," *Trans. China Electrotech. Soc.*, vol. 34, no. S2, pp. 637–645, Nov. 2019.

[24] L. C. Deng, X. D. Zhao, and J. Liu, "Retrospect and prospects of the electricity system reform," *Energy Institutional Reform Revolution*, vol. 46, no. 3, pp. 96–103, Mar. 2024.

[25] X. Gao, C. M. Yang, Z. Q. Zhu, Y. H. Wu, Y. P. Chen, and Z. Y. Mu, "A mini-review on trading mechanisms of emerging joint energy markets with high shares of renewables," *Front. Energy Res.*, vol. 12, pp. 1391813, Apr. 2024.

[26] National Development and Reform Commission, National Energy Administration. (2024, Feb.). Notice on establishing and improving the price mechanism for the power auxiliary service market. [Online]. Available: https://www.gov.cn/zhengce/zhengceku/202402/content_6931026.htm.

[27] C. Y. Chen, C. K. Huang, J. X. Wang, X. M. Dai, and Y. Wang, "Multi-time-scale frequency regulation market clearing and dispatch strategy considering wind power uncertainty," *Trans. China Electrotech. Soc.*, vol. 39, no. 21, pp. 6804–6818, Nov. 2024.

[28] X. R. Xie, N. J. Ma, W. Liu, W. Zhao, P. Xu, and H. Z. Li, "Functions of energy storage in renewable energy dominated power systems: review and prospect," *Proc. CSEE*, vol. 43, no. 1, pp. 158–168, Jan. 2023.

[29] C. Wang, W. Wei, L. J. Chen, Y. Gong, and S. W. Mei, "An hourly-resolution capacity sharing market for generation-side clustered renewable-storage plants," *Appl. Energy*, vol. 380, pp. 124964, Feb. 2025.

[30] J. C. Xiao, Y. Meng, L. Li, S. Fan, G. Y. He, and Z. Y. Li, "Market equilibrium with strategic pricing and strategic constraints in renewable energy: the role of private energy storage," *Front. Energy Res.*, vol. 12, pp. 1346528, Mar. 2024.

[31] G. Brusco, D. Menniti, A. Pinnarelli, and N. Sorrentino, "Renewable energy community with distributed storage optimization to provide energy sharing and additional ancillary services," *Sustainable Energy, Grids Networks*, vol. 36, pp. 101173, Dec. 2023.

[32] J. H. Li, T. Hou, G. Mu, G. G. Yan, and C. P. Li, "Optimal control strategy for energy storage considering wind farm scheduling plan and modulation frequency limitation under electricity market environment," *Trans. China Electrotech. Soc.*, vol. 36, no. 9, pp. 1791–1804, May 2021.

Junhui Li (Senior Member, IEEE) received the Ph.D. degree in Electrical Engineering from North China Electric Power University, China, in 2012. He is a Professor and a Doctoral supervisor at Northeast Electric Power University. His research interests include grid-connected operation and control of wind power and photovoltaic power, and large-scale energy storage and its applications.

Qinglin Sui received the Bachelor's degree in Electrical Engineering from Northeast Electric Power University in 2024. He is currently a master's candidate at Northeast Electric Power University, China. His research interest focuses on the secondary frequency regulation of renewable power plants assisted by energy storage.

Wenbo Si received his M.Sc. degree in Electrical Engineering from Northeast Electric Power University in 2024. He is currently employed by Suichang County Power Supply Company, State Grid Zhejiang Electric Power Co., Ltd. His research interests focus on frequency regulation strategies for power systems with high penetration of renewable energy.

Xingxu Zhu received the Ph.D. degree in Electrical Engineering from Shandong University, Jinan, China, in 2020. He is currently an Associate Professor with the Department of Electrical Engineering at Northeast Electric Power University. His research interests cover distributed optimization of power systems, as well as distributed control of energy storage systems.

David Campos-Gaona (Senior Member, IEEE) received the B.E. degree in electronic engineering and the M.Sc. and Ph.D. degrees in electrical engineering from the Instituto Tecnológico de Morelia, Morelia, Mexico, in 2004, 2007, and 2012, respectively. From 2014 to 2016, he was a Post-Doctoral Research Fellow with the Department of Electrical and Computer Engineering, The University of British Columbia, Vancouver, BC, Canada. Since 2016, he has been with the University of Strathclyde, Glasgow, U.K., first as a Research Associate and currently as a Senior Lecturer. His research interests include wind farm power integration, HVDC transmission systems, variable frequency systems, and real-time digital control of power-electronic-based devices.

Fulin Fan (Member, IEEE) received the B.Eng. degree in electrical engineering and automation from the North China Electric Power University, Baoding, China, in 2012, and the Ph.D. degree in electronic and electrical engineering from the University of Strathclyde, Glasgow, U.K., in 2018. He was a Research Assistant from 2016 to 2018 and a Research Associate from 2018 to 2024 with the University of Strathclyde. He is currently an Associate Professor with the School of Electrical Engineering and Automation, Harbin Institute of Technology, Harbin, China. His research interests include integrated energy system scheduling and planning, real-time thermal rating for overhead lines, and transportation electrification.

Ziyun Zong received his Master's degree in Electrical Engineering from Northeast Electric Power University in 2026. His research interest focuses on the secondary frequency regulation of thermal power units assisted by energy storage.

Cuiping Li received the Ph.D. degree in Electrical Engineering from Harbin Institute of Technology, China, in 2013. She is a Associate Professor and a Master supervisor at Northeast Electric Power University. Her research interests include grid-connected operation and control of wind power and photovoltaic power, and large-scale energy storage and its applications.